JCI The Journal of Clinical Investigation

In vivo hematopoietic stem cell gene therapy ameliorates murine thalassemia intermedia

Hongjie Wang, … , Evangelia Yannaki, André Lieber

J Clin Invest. 2019;129(2):598-615. https://doi.org/10.1172/JCI122836.

Research Article **Hematology** **Therapeutics**

Current thalassemia gene therapy protocols require the collection of hematopoietic stem/progenitor cells (HSPCs), in vitro culture, lentivirus vector transduction, and retransplantation into myeloablated patients. Because of cost and technical complexity, it is unlikely that such protocols will be applicable in developing countries, where the greatest demand for a β-thalassemia therapy lies. We have developed a simple in vivo HSPC gene therapy approach that involves HSPC mobilization and an intravenous injection of integrating HDAd5/35++ vectors. Transduced HSPCs homed back to the bone marrow, where they persisted long-term. HDAd5/35++ vectors for in vivo gene therapy of thalassemia had a unique capsid that targeted primitive HSPCs through human CD46, a relatively safe SB100X transposase–based integration machinery, a micro-LCR–driven γ-globin gene, and an MGMT(P140K) system that allowed for increasing the therapeutic effect by short-term treatment with low-dose O^6-benzylguanine plus bis-chloroethylnitrosourea. We showed in "healthy" human CD46–transgenic mice and in a mouse model of thalassemia intermedia that our in vivo approach resulted in stable γ-globin expression in the majority of circulating red blood cells. The high marking frequency was maintained in secondary recipients. In the thalassemia model, a near-complete phenotypic correction was achieved. The treatment was well tolerated. This cost-efficient and "portable" approach could permit a broader clinical application of thalassemia gene therapy.

In vivo hematopoietic stem cell gene therapy ameliorates murine thalassemia intermedia

Hongjie Wang,[1] Aphrodite Georgakopoulou,[2,3] Nikoletta Psatha,[1] Chang Li,[1] Chrysi Capsali,[3] Himanshu Bhusan Samal,[4] Achilles Anagnostopoulos,[2] Anja Ehrhardt,[5] Zsuzsanna Izsvák,[4] Thalia Papayannopoulou,[6] Evangelia Yannaki,[2] and André Lieber[1,7]

[1]Division of Medical Genetics, Department of Medicine, University of Washington, Seattle, Washington, USA. [2]Gene and Cell Therapy Center, Hematology Department, George Papanicolaou Hospital, Thessaloniki, Greece. [3]Aristotle University of Thessaloniki, Thessaloniki, Greece. [4]Max Delbrück Center for Molecular Medicine, Berlin, Germany. [5]Witten/Herdecke University, Witten, Germany. [6]Division of Hematology, Department of Medicine, and [7]Department of Pathology, University of Washington, Seattle, Washington, USA.

Current thalassemia gene therapy protocols require the collection of hematopoietic stem/progenitor cells (HSPCs), in vitro culture, lentivirus vector transduction, and retransplantation into myeloablated patients. Because of cost and technical complexity, it is unlikely that such protocols will be applicable in developing countries, where the greatest demand for a β-thalassemia therapy lies. We have developed a simple in vivo HSPC gene therapy approach that involves HSPC mobilization and an intravenous injection of integrating HDAd5/35++ vectors. Transduced HSPCs homed back to the bone marrow, where they persisted long-term. HDAd5/35++ vectors for in vivo gene therapy of thalassemia had a unique capsid that targeted primitive HSPCs through human CD46, a relatively safe SB100X transposase–based integration machinery, a micro-LCR–driven γ-globin gene, and an MGMT(P140K) system that allowed for increasing the therapeutic effect by short-term treatment with low-dose *O*^{6}-benzylguanine plus bis-chloroethylnitrosourea. We showed in "healthy" human CD46–transgenic mice and in a mouse model of thalassemia intermedia that our in vivo approach resulted in stable γ-globin expression in the majority of circulating red blood cells. The high marking frequency was maintained in secondary recipients. In the thalassemia model, a near-complete phenotypic correction was achieved. The treatment was well tolerated. This cost-efficient and "portable" approach could permit a broader clinical application of thalassemia gene therapy.

Introduction

Thalassemia is one of the most common inherited diseases in humans worldwide (1), resulting from absent (β0/β0) or deficient (β+/β+) β-globin chain synthesis. Approximately 60,000 children are born annually with β-thalassemia major. Without treatment, children with thalassemia major die in their first to second decade of life. In the absence of sufficient β-globin chain synthesis for hemoglobin tetramer formation, excess α-globin chains precipitate and form inclusions that cause the premature death of late erythroblasts in the bone marrow or reduce the half-life of circulating erythrocytes, generating the major hematological hallmarks of β-thalassemia, ineffective erythropoiesis and erythrocyte death. The resulting anemia stimulates the expansion of the hematopoietic compartment, producing erythroid hyperplasia and extramedullary hematopoiesis.

The major treatment modalities for β-thalassemia major consist of supportive care with lifelong transfusions of red blood cells (RBCs) and chelation to remove excess iron; or curative treatment with transplantation of allogeneic hematopoietic stem/progenitor cells (HSPCs). For patients lacking a well-matched donor or at risk to undergo an allogeneic HSPC transplantation, lentiviral vector wild-type β-globin or fetal γ-globin gene therapy has the potential for a cure bypassing the immunological risks of allogeneic transplantation. HSPC gene therapy with SIN-lentiviral globin vectors, incorporating micro-LCR cassettes, rescued β-thalassemia and sickle cell disease (SCD) phenotypes in animal models and in patient cells in vitro (reviewed in ref. 2). Based on this, a number of clinical trials for thalassemia and SCD are currently ongoing in Europe, Asia, and the United States (2–5). While the data from these trials so far demonstrate long-term transfusion independence for the majority of patients having a β+ genotype, the cure of β0/β0 thalassemia still remains a challenge.

Despite the encouraging clinical results, current thalassemia gene therapy protocols are complex, involving the collection of HSPCs from donors/patients by leukapheresis, in vitro culture, transduction with lentivirus vectors carrying a β- or γ-globin expression cassette, and retransplantation into patients conditioned with full myeloablation. Besides the technical complexity, other disadvantages of this approach include (a) the necessity for culture in the presence of multiple cytokines, which can affect the pluripotency of hematopoietic stem cells (HSCs) and their engraftment potential; (b) the requirement for myeloablative regimens, as myeloablation in patients with chronic, nonmalignant diseases and preexisting organ damage, such as those with hemoglobinopathies, represents a critical risk factor associated with considerable hematopoietic and nonhematopoietic, early or late toxicity; and (c) the cost of the approach. A similarly complex HSPC gene therapy product for SCID due to adenosine deaminase deficiency (ADA-SCID) (Strimvelis) is currently sold

Authorship note: HW and AG contributed equally to this work.
Conflict of interest: The authors have declared that no conflict of interest exists.

Submitted: June 13, 2018; **Accepted:** November 6, 2018.
Reference information: *J Clin Invest*. 2019;129(2):598–615.
https://doi.org/10.1172/JCI122836.

for $600,000–$900,000 per patient. The fact that thalassemia is prevalent in resource-poor countries demands a simpler and cheaper therapy approach.

We developed a minimally invasive and readily translatable approach for in vivo HSPC gene delivery without leukapheresis, myeloablation, and HSPC transplantation (6–8). It involves injections of G-CSF/AMD3100 to mobilize HSPCs from the bone marrow into the peripheral bloodstream and the intravenous injection of an integrating, helper-dependent adenovirus (HDAd5/35++) vector system. HDAd5/35++ vectors target human CD46, a receptor that is expressed on primitive HSCs (6). Transgene integration is achieved, in a random pattern, by a hyperactive Sleeping Beauty transposase (SB100X) (9). We demonstrated in mouse models, using GFP as a reporter gene, that HSPCs transduced in the periphery home back to the bone marrow, where they persist and stably express the reporter long-term in in vivo–transduced mice and secondary recipients (6).

Given the high level of transgene marking required in order to phenotypically correct thalassemia, we further optimized our in vivo HSPC transduction approach by inserting an MGMT(P140K) expression cassette into HDAd5/35++ vectors. This allows for in vivo selection of gene-corrected progenitors with low doses of methylating agents, e.g., O^6-benzylguanine (O^6BG) plus bischloroethylnitrosourea (BCNU) or temozolomide (10–12). We have previously shown that the combined in vivo transduction/selection approach was safe and resulted in stable GFP expression in up to 80% of peripheral blood cells, a level that was maintained in secondary recipients, indicating the stable transduction of self-renewing, multilineage, long-term repopulating HSCs (13).

Here we tested the in vivo HSPC gene therapy approach using an integrating HDAd5/35++ vector expressing the human γ-globin gene in "healthy" human CD46–transgenic (CD46tg) mice and, as a proof of concept, in a mouse model for thalassemia intermedia ($CD46^{+/+}$/Hbbth-3 mice).

Results

In vivo HSPC transduction with subsequent in vivo selection in CD46tg mice results in stable γ-globin expression in the majority of peripheral RBCs. The therapeutic HDAd5/35++ vector contains the human γ-globin gene under the control of 5-kb "micro" β-globin LCR/β-promoter for efficient expression in erythrocytes as well as an MGMT(P140K) expression cassette (Figure 1A, HDAd-γ-globin/mgmt). CD46tg mice are homozygous for the human CD46 locus expressing the HDAd5/35++ receptor CD46 in a pattern and at a level similar to that in humans and are therefore a model for in vivo HSPC transduction studies (6, 14). The goal of our studies in "healthy" CD46tg mice was to analyze the level, kinetics, and distribution of human γ-globin on mouse cells and the safety of the approach. Animals were mobilized with G-CSF/AMD3100 and then intravenously injected with HDAd-γ-globin/mgmt and the SB100X-expressing HDAd-SB vector. Three cycles of O^6BG/BCNU treatment were initiated 4 weeks after vector injection, and mice were followed until week 18 after injection of the vectors (Figure 1B). First, we analyzed human γ-globin expression in RBCs (Figure 1C). The levels before the start of in vivo selection (week 4 after transduction) were only marginally above background. The percentage of γ-globin$^+$ cells started to increase after the second round of selection and reached levels above 80% after the third round. The percentage of γ-globin–expressing cells was approximately 7- to 10-fold higher in erythroid Ter119$^+$ cells versus nonerythroid Ter119$^-$ cells in peripheral blood and bone marrow (Figure 1D). We used HPLC to measure the level of γ-globin protein in comparison with the adult mouse α- and β-globin chains (Figure 1E and Supplemental Figure 1; supplemental material available online with this article; https://doi.org/10.1172/JCI122836DS1). At week 18, these levels reached 10%–15% of adult mouse α-globin and β-major globin and approximately 25% of mouse β-minor globin. This was confirmed on the mRNA level by quantitative reverse transcription PCR (RT-qPCR), where human γ-globin mRNA was approximately 13% of mouse β-major mRNA (Figure 1F). To further demonstrate that primitive, long-term repopulating HSCs were transduced, we transplanted lineage-depleted (Lin$^-$) bone marrow cells from in vivo–transduced/selected mice into irradiated C57BL/6 mice. Engraftment levels analyzed in peripheral blood, bone marrow, and spleen were greater than 95% and stable over an observation period of 20 weeks (Supplemental Figure 2, A and B). Human γ-globin levels (compared with mouse α-globin) were similar in ("primary") in vivo–transduced mice (analyzed at week 18 after transduction) and secondary recipients analyzed at weeks 14 and 20 after transplantation (Supplemental Figure 2C).

The in vivo HSPC transduction/selection approach does not change the SB100X-mediated random transgene integration pattern and does not alter hematopoiesis. We previously showed that in vivo transduction with the hybrid transposon/SB100X HDAd5/35++ system resulted in random transgene integration in HSPCs (6). To evaluate the effect of O^6BG/BCNU in in vivo selection, we analyzed transgene integration in bone marrow Lin$^-$ cells at the end of the study, i.e., at week 20 in secondary recipients. Linear amplification–mediated PCR (LAM-PCR) followed by deep sequencing showed a random distribution pattern of integration sites in the mouse genome (Figure 2A). Data pooled from 5 mice demonstrated 2.23% integration into exons, 31.58% into introns, 65.17% into intergenic regions, and 1.04% into untranslated regions (Figure 2B). The level of randomness of integration was 99% without preferential integration in any given window of the whole mouse genome (Figure 2C). This indicates that in vivo selection and further expansion of cells in secondary recipients did not result in the emergence of dominant integration sites (Figure 2D). We measured, by qPCR, on average two γ-globin cDNA copies per bone marrow cell in a population containing both transduced and nontransduced cells. We then quantified the integrated transgene copy number on a single-cell level. To do this, we plated bone marrow Lin$^-$ cells from week 18 mice in methylcellulose, isolated individual progenitor colonies, and performed qPCR on genomic DNA. In transgene-positive colonies (n = 113), 86.7% of colonies had 2 or 3 integrated copies (Figure 2E and Supplemental Figure 3). Four copies were found in 6.2% of colonies, 8 copies in 1.78%. 0.88% of colonies had either 13, 10, 7, 6, or 5 integrated vector copies.

No alterations in blood cell counts were found at the end the study (week 18) (Figure 3A). Analysis of RBC parameters did not show abnormalities (Figure 3, B and C). Composition of Lin$^+$ fractions in the bone marrow was similar in mice before and after

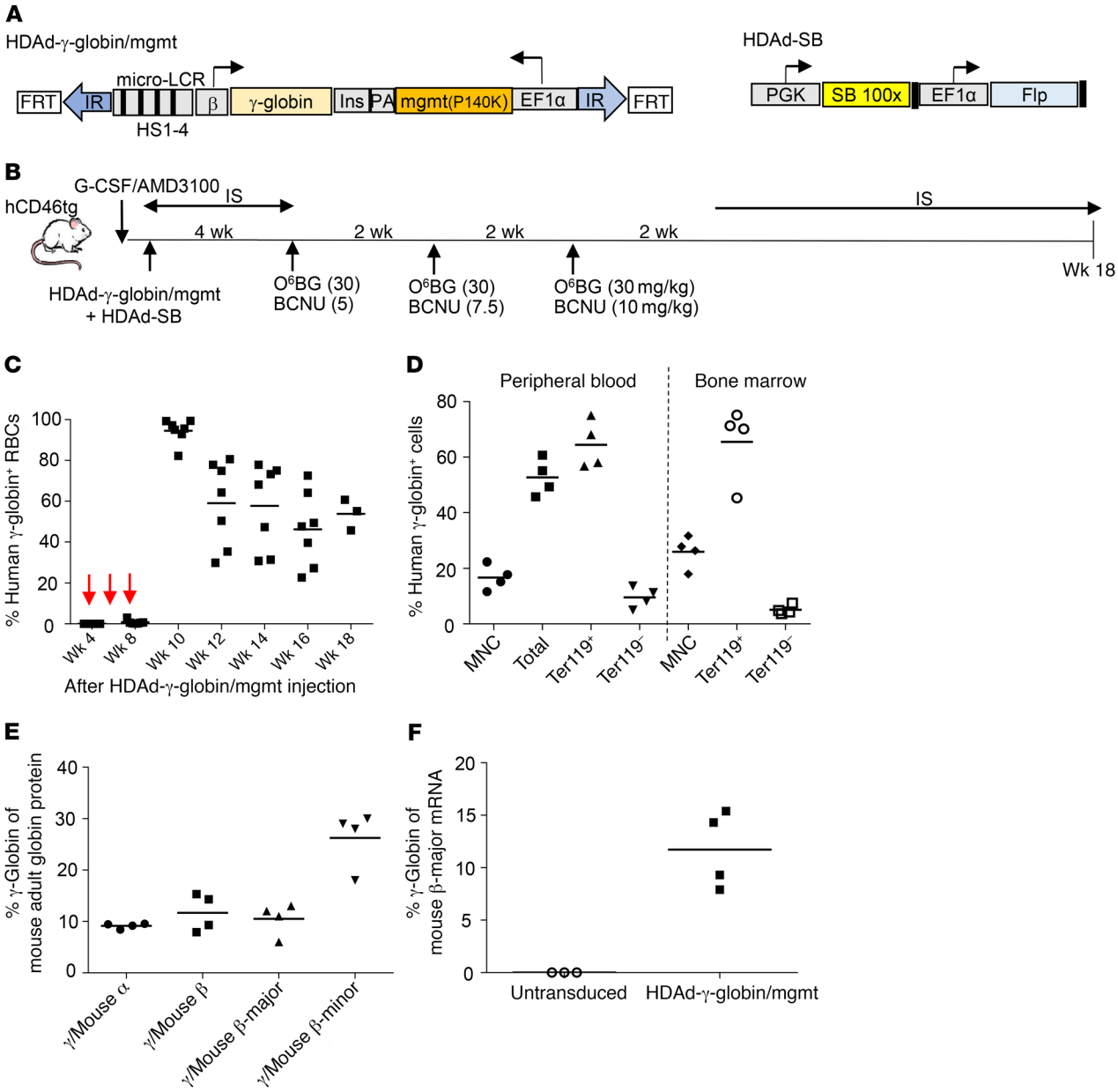

Figure 1. Integrating HDAd5/35++ vector for HSPC gene therapy of hemoglobinopathies. (**A**) Vector structure. In HDAd-γ-globin/mgmt, the 11.8-kb transposon is flanked by inverted transposon repeats (IR) and FRT sites for integration through a hyperactive Sleeping Beauty transposase (SB100X) provided from the HDAd-SB vector (right panel). The γ-globin expression cassette contains a 4.3-kb version of the β-globin LCR consisting of 4 DNase hypersensitivity (HS) regions and the 0.7-kb β-globin promoter. The 76-Ile *HBG1* gene including the 3′-UTR (for mRNA stabilization in erythrocytes) was used. To avoid interference between the LCR/β-promoter and EF1A promoter, a 1.2-kb chicken HS4 chromatin insulator (Ins) was inserted between the cassettes. The HDAd-SB vector contains the gene for the activity-enhanced SB100X transposase and Flpe recombinase under the control of the ubiquitously active PGK and EF1A promoters, respectively. (**B**) In vivo transduction of mobilized CD46tg mice. HSPCs were mobilized by s.c. injections of human recombinant G-CSF for 4 days followed by 1 s.c. injection of AMD3100. Thirty and 60 minutes after AMD3100 injection, animals were injected i.v. with a 1:1 mixture of HDAd-γ-globin/mgmt plus HDAd-SB (2 injections, each 4×10^{10} viral particles). Mice were treated with immunosuppressive (IS) drugs for the next 4 weeks to avoid immune responses against the human γ-globin and MGMT(P140K). O^6-BG/BCNU treatment was started at week 4 and repeated every 2 weeks 3 times. With each cycle the BCNU concentration was increased, from 5 to 7.5 to 10 mg/kg. Immunosuppression was resumed 2 weeks after the last O^6-BG/BCNU injection. (**C**) Percentage of human γ-globin$^+$ peripheral RBCs measured by flow cytometry. (**D**) Percentage of human γ-globin$^+$ cells in peripheral blood mononuclear cells (MNC), total cells, erythroid Ter119$^+$ cells, and nonerythroid Ter119$^-$ cells. (**E**) Percentage of human γ-globin protein compared with adult mouse globin chains (α, β-major, β-minor) measured by HPLC in RBCs at week 18. (**F**) Percentage of human γ-globin mRNA compared with adult mouse β-major globin mRNA measured by RT-qPCR in total in peripheral blood cells at week 18. Mice that did not receive any treatment were used as a control. In **C**–**F**, each symbol represents an individual animal.

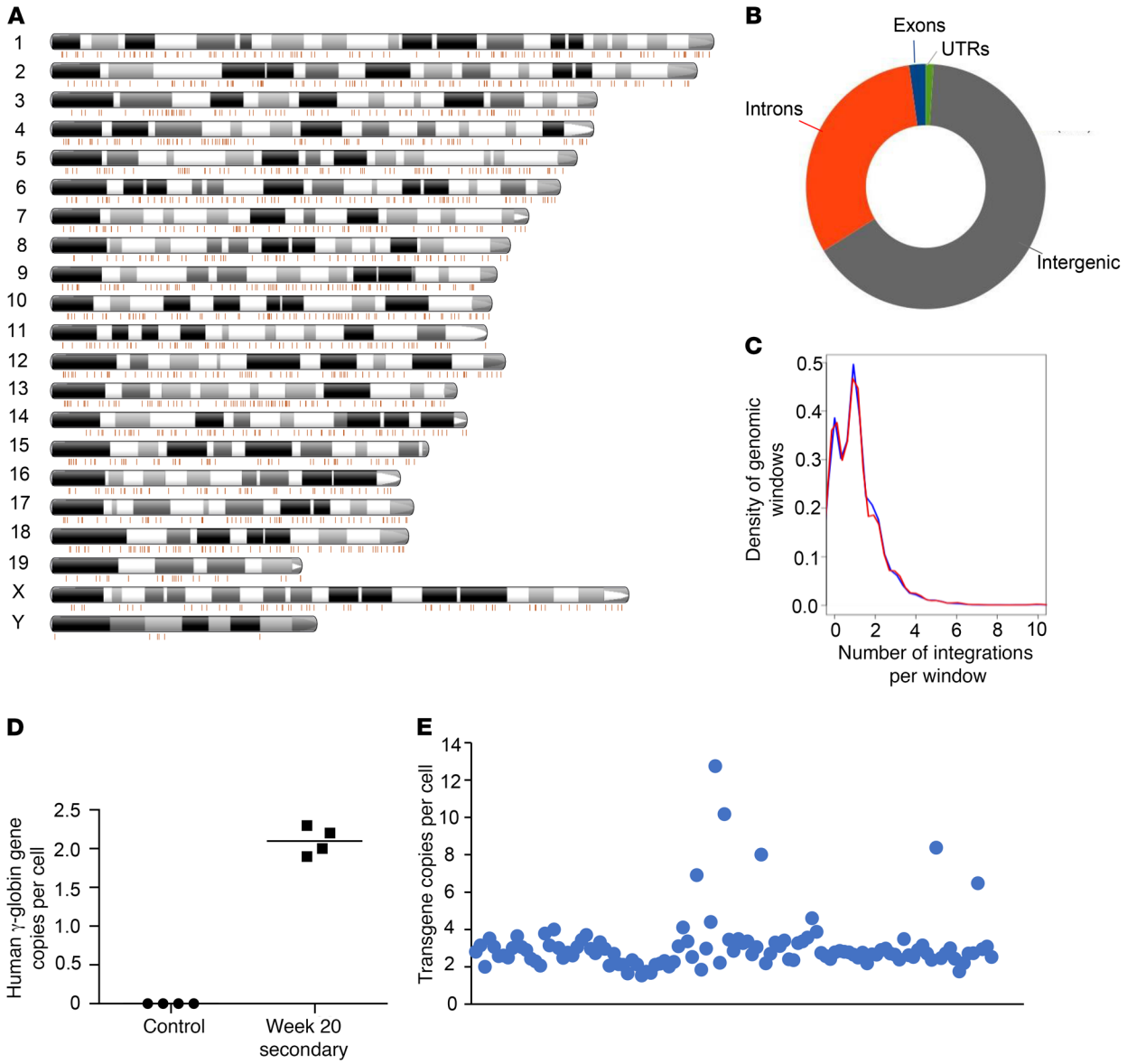

Figure 2. Analysis of transgene integration in bone marrow cells of week 20 secondary recipients. (**A**) Localization of integration sites on mouse chromosomes of bone marrow cells. Shown is a representative mouse. Each line is an integration site. The number of integration sites in this sample is 2,197. (**B**) Distribution of integrations in genomic regions. Integration site data from 5 mice were pooled and used to generate the graph. (**C**) The number of integrations overlapping with continuous genomic windows and randomized mouse genomic windows and size was compared. Pooled data were used as in **B**. The Pearson's χ^2 test *P* value for similarity is 0.06381, implying that the integration pattern is close to random. (**D**) Transgene copy numbers. Genomic DNA from total bone marrow cells from untransduced control mice and week 20 secondary recipients was subjected to qPCR with human γ-globin–specific primers. Shown is the copy number per cell for individual animals. Each symbol represents an individual animal. (**E**) Transgene copy numbers in individual clonal progenitor colonies. Bone marrow Lin^- cells were plated in methylcellulose, and individual colonies were picked 15 days later. qPCR was performed on genomic DNA. Shown is normalized qPCR signal in individual colonies expressed as transgene copy number per cell (n = 113). Each symbol represents the copy number in an individual colony derived from a single cell.

treatment (week 18) mice (Figure 3D). The levels of $Lin^-Sca1^+cKit^+$ (LSK) HSPCs (Figure 3D, last lane) and progenitor colony-forming cells (Figure 3E) were also comparable in both groups.

Generation of the CD46$^{+/+}$/Hbbth-3 mouse model expressing human CD46 and resembling human thalassemia intermedia. HDAd5/35++ vectors require human CD46 for infection. In order to develop a thalassemic mouse model for in vivo HSPC transduction studies, CD46tg (CD46$^{+/+}$) mice were bred with Hbbth-3 mice heterozygous for the mouse Hbb-β1 and -β2 gene deletion (15). (The homozygous state is lethal in utero or early postnatally.) Hbbth-3 mice represent a viable form of thalassemia, resembling human thalassemia intermedia. F_1 hybrid mice were backcrossed with CD46$^{+/+}$ mice to generate CD46$^{+/+}$/Hbbth-3 mice (Supplemental Figure 4). These mice displayed a thalassemic phenotype. Compared with parental CD46tg mice, CD46$^{+/+}$/Hbbth-3 mice had significantly decreased RBC numbers (7.1 ± 0.1 vs. 8.63 ± 0.29 M/μl); lower hemoglobin (9.7 ± 0.18 vs. 13.9 ± 0.63 g/dl), hematocrit (30.7% ± 0.46% vs. 41.7% ± 1.48%), mean corpuscular

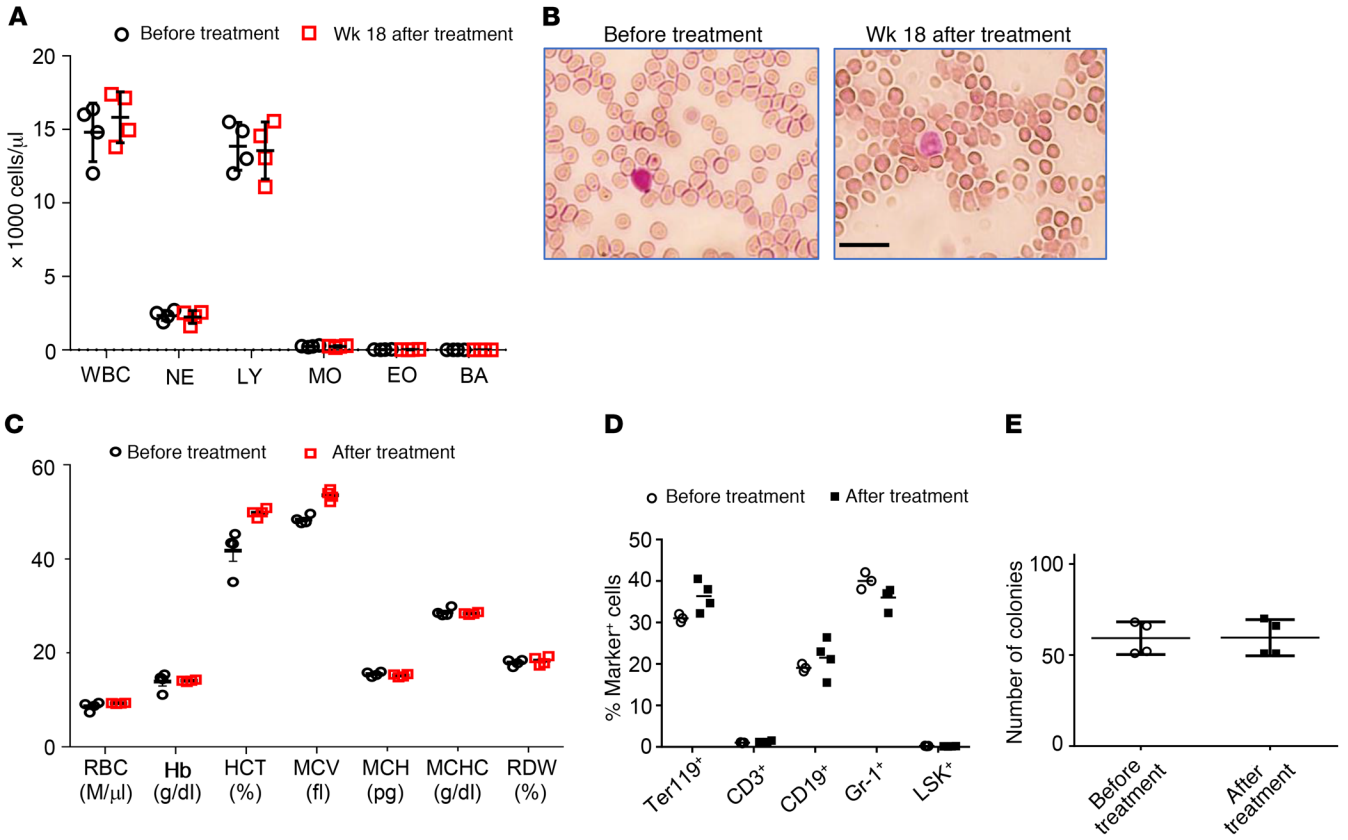

Figure 3. Hematological parameter after in vivo HSPC transduction/selection in CD46tg mice (week 18 after HDAd injection). (**A**) WBC counts. (**B**) Representative blood smears from an untreated mouse and a mouse at week 18 after HDAd-γ-globin/mgmt plus HDAd-SB injection. Scale bar: 20 μm. Nuclei of WBCs stain purple. (**C**) Hematological parameters. Hb, hemoglobin; HCT, hematocrit; MCV, mean corpuscular volume; MCH, mean corpuscular hemoglobin; MCHC, mean corpuscular hemoglobin concentration; RDW, red cell distribution width. $n \geq 3$, $^*P < 0.05$. Statistical analysis was performed using 2-way ANOVA. (**D**) Cellular bone marrow composition in naive mice (control) and treated mice sacrificed at week 18. Shown is the percentage of lineage marker–positive cells (Ter119$^+$, CD3$^+$, CD19$^+$, and Gr-1$^+$ cells) and HSPCs (LSK cells). (**E**) Colony-forming potential of bone marrow Lin$^-$ cells harvested at week 18 after in vivo transduction. Shown is the number of colonies that formed after plating of 2,500 Lin$^-$ cells. In **A** and **C**–**E**, each symbol represents an individual animal. NE, neutrophils; LY, lymphocytes; MO, monocytes; BA, basophils.

hemoglobin (13.9 ± 0.14 vs. 16.1 ± 0.23 g/dl), and mean corpuscular volume (43.03 ± 0.22 vs. 48.35 ± 0.9 fl); and increased RBC distribution width (42.9% ± 0.29% vs. 25.3% ± 0.79%); and showed overt reticulocytosis (42.4% ± 1.43% vs. 11.8% ± 3.7%) (Figure 4A). The red cell morphology in blood smears was characterized by hypochromia, widely varying sizes and shapes (anisopoikilocytosis), and cell fragmentation, similarly to the morphology of the Hbbth-3 mouse blood smears and in sharp contrast to the normocytic red cell appearance of CD46tg mice (Figure 4B). Likewise, histological analysis of liver and spleen from CD46$^{+/+}$/Hbbth-3 mice revealed foci of extramedullary hemopoiesis containing clusters of erythroid precursors or megakaryocytes (Figure 4C, bottom left and bottom middle panels), while Perls' staining demonstrated marked parenchymal iron deposition (Figure 4C, bottom right panel) as opposed to absent or limited extramedullary hemopoiesis and iron accumulation in tissue sections from parental CD46tg mice (Figure 4C, top panels). These characteristics of CD46$^{+/+}$/Hbbth-3 mice recapitulate the human disease and support the validity of such a model for subsequent experiments. Notably, the thalassemic phenotype in the CD46$^{+/+}$/Hbbth-3 model was also characterized by quantitative differences in lineages other than the erythroid lineage, as indicated by the elevated numbers of total WBCs (Supplemental Figure 5).

HSPC in vivo transduction with HDAd-γ-globin/mgmt plus HDAd-SB followed by in vivo selection in CD46$^{+/+}$/Hbbth-3 mice results in high, stable, and long-term expression of γ-globin. We next determined whether our in vivo transduction approach could ameliorate the characteristic disease parameters of the CD46$^{+/+}$/Hbbth-3 thalassemia mouse model. A modified G-CSF/AMD3100 mobilization scheme that was previously validated in Hbbth-3 mice (16) yielded high numbers of LSK cells in the peripheral blood 1 hour after the last plerixafor (AMD3100) injection (Supplemental Figure 6), i.e., at the time point when HDAd-γ-globin/mgmt and HDAd-SB were injected intravenously. Mice received immunosuppression to avoid responses against the human γ-globin and MGMT proteins (Supplemental Figure 7). Considering a report that after ex vivo lentivirus vector gene therapy, genetically corrected erythroblasts have a survival advantage and undergo in vivo selection in Hbbth-3 mice (17), we initially planned to conduct the study without O^{6}BG/BCNU treatment. Average γ-globin$^+$ RBC percentages reached 31.19% ± 2.7% at week 8 after in vivo transduction of CD46$^{+/+}$/Hbbth-3

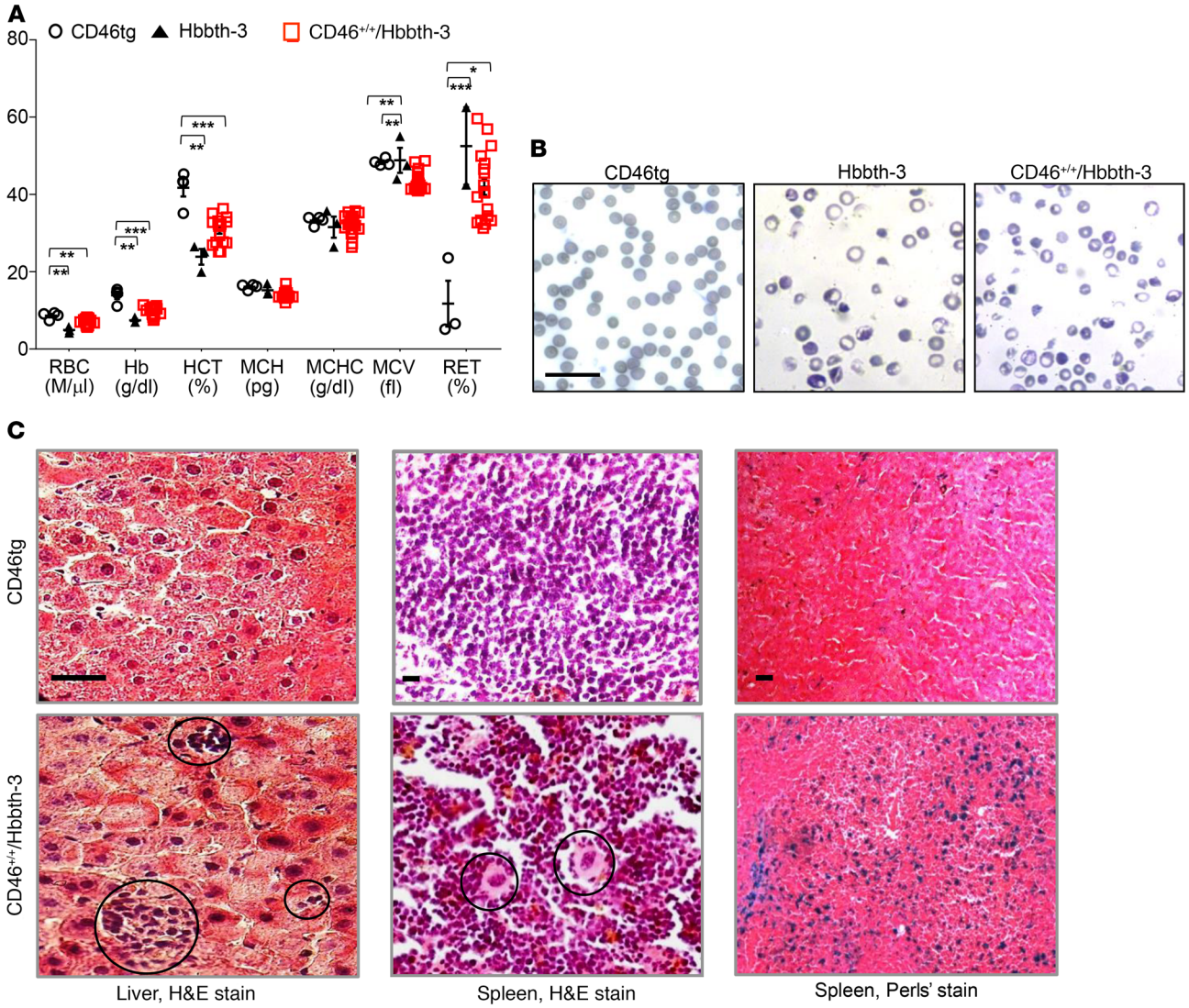

Figure 4. Phenotype of the CD46$^{+/+}$/Hbbth-3 mouse thalassemia model. (**A**) Hematological parameters of CD46$^{+/+}$/Hbbth-3 mice (n = 7) as compared with CD46tg (n = 3) and Hbbth-3 mice (n = 3). Each symbol represents an individual animal. *$P \le 0.05$, **$P \le 0.0002$, ***$P \le 0.00003$. Statistical analysis was performed using 2-way ANOVA. RET, reticulocytes. (**B**) Representative peripheral blood smears after staining with May-Grünwald/Giemsa. Scale bar: 20 μm. (**C**) Extramedullary hemopoiesis by H&E staining in liver and spleen sections of CD46$^{+/+}$/Hbbth-3 mice (bottom left 2 panels) as compared with spleen and liver sections of CD46tg mice (top left 2 panels). Scale bars: 20 μm. Clusters of erythroblasts in the liver are indicated in the bottom left panel. Circles in the bottom middle panel mark megakaryocytes in the spleen. Iron deposition (granular bluish deposits) by Perls' staining in the spleen are shown in the top right panel for CD46tg and the bottom right panel for CD46$^{+/+}$/Hbbth-3 mice. Scale bar: 25 μm.

mice but declined to 13.14% ± 0.4% by week 16. At this time, we split the mice into 2 groups. Half of the mice were used for blood and bone marrow analysis (group 1: without in vivo selection) and as donors for secondary recipients, while the study was continued with the other group involving O^{6}BG/BCNU in vivo selection (group 2: with in vivo selection) (see Supplemental Figure 7). At week 16, group 1 showed γ-globin expression in approximately 13% of peripheral RBCs (Figure 5, A and B). This level of γ-globin marking resulted in a significant reduction in the percentage of peripheral blood reticulocytes (Figure 5C, last lane). However, it did not suffice to improve other RBC parameters, including RBC morphology and extramedullary hemopoiesis (Figure 5, C and D). The level of primary γ-globin marking was maintained over 20 weeks in secondary C57BL/6 recipients that were myelo-conditioned with busulfan before transplantation (Figure 5, E and F). This indicates that long-term-repopulating HSPCs were transduced.

In group 2, 4 cycles of in vivo selection resulted in a 6-fold increase in the percentage γ-globin$^+$ RBCs reaching an average of 76% at week 29 (Figure 6A). γ-Globin expression was erythroid-specific as indicated by analysis of γ-globin expression in gated or immunomagnetically isolated Ter119$^+$ erythroid cells by flow cytometry as compared with Ter119$^-$ cells (Figure 6, B and C). In agreement with other studies (17, 18), selection occurred at the level of (nucleated and proliferating erythroid) progenitors before they exit the bone marrow (or spleen) and lose their nucleus. This is reflected in an increase of γ-globin$^+$Ter119$^+$ cells in the bone marrow and spleen that occurred predominantly

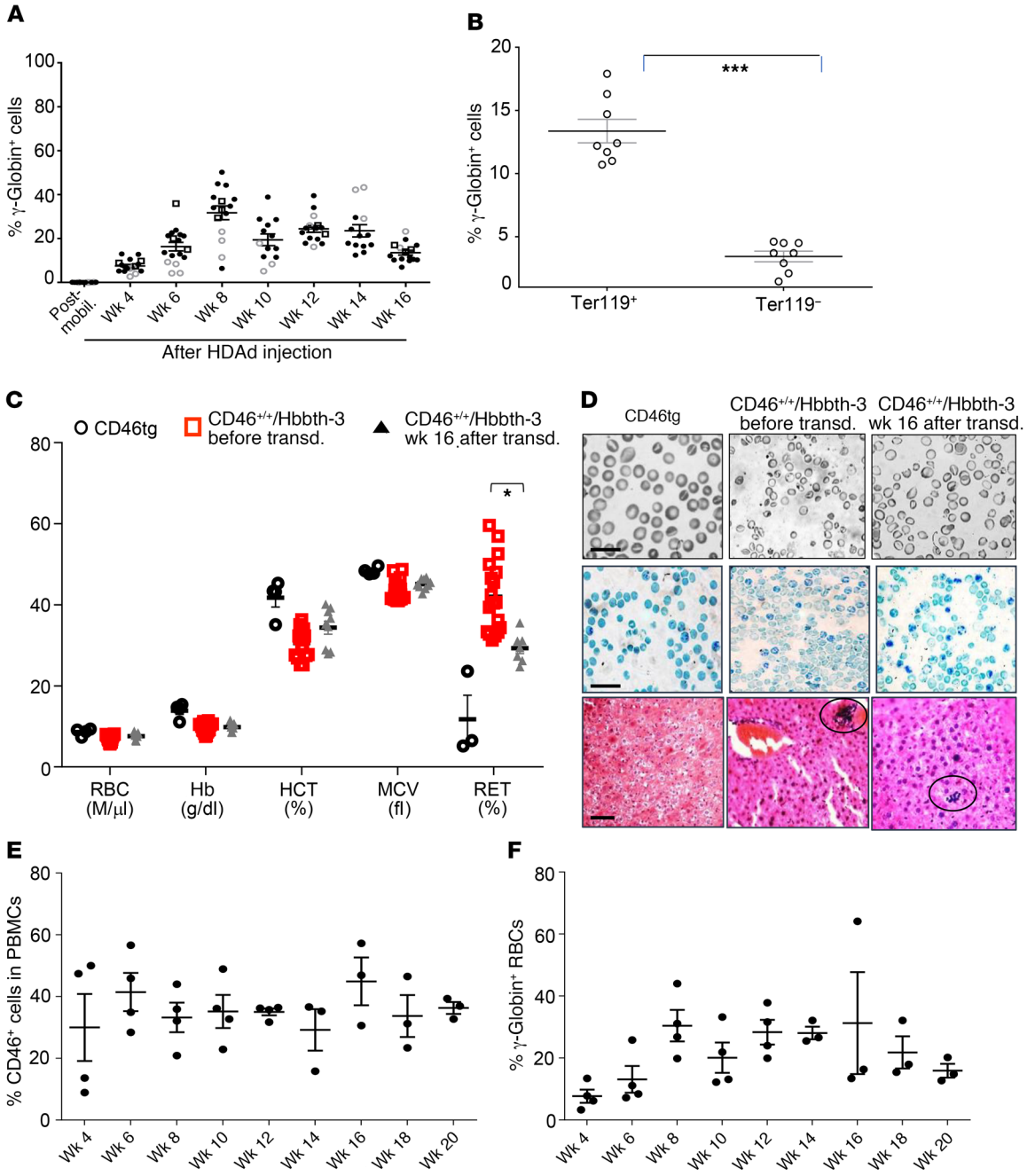

Figure 5. Analysis of in vivo–transduced CD46$^{+/+}$/Hbbth-3 mice that did not receive O^{6}BG/BCNU treatment. (**A**) Percentage of human γ-globin in peripheral RBCs measured by flow cytometry. The experiment was performed 3 times, indicated by different symbol shapes. (**B**) γ-Globin expression in erythroid (Ter119$^+$) and nonerythroid (Ter119$^-$) blood cells. ***$P \le 0.00003$ by 1-way ANOVA test. (**C**) RBC analysis of healthy (CD46tg) mice ($n = 3$), CD46$^{+/+}$/Hbbth-3 mice prior to mobilization and in vivo transduction ($n = 14$), and CD46$^{+/+}$/Hbbth-3 mice that underwent in vivo transduction and were analyzed at week 16 ($n = 8$). *$P \le 0.05$. Statistical analysis was performed using 2-way ANOVA. (**D**) Histological phenotype. Top: Blood smears. Middle: Supravital stain of peripheral blood smears with Brilliant cresyl blue for reticulocyte detection. The percentages of positively stained reticulocytes in representative smears were: for CD46tg, 8% ± 0.8%; for CD46$^{+/+}$/Hbbth-3 before transduction, 39% ± 1.3%; and for CD46$^{+/+}$/Hbbth-3 week 16 after transduction, 26% ± 0.45%. Bottom: Extramedullary hemopoiesis. Scale bars: 20 μm. (**E** and **F**) Analysis of secondary recipients. Total bone marrow from week 16 in vivo–transduced mice was transplanted into C57BL/6 mice that received sublethal busulfan preconditioning. Mice received immunosuppression during the period of observation. (**E**) Engraftment based on the percentage of human CD46$^+$ (hCD46$^+$) PBMCs. (C57BL/6 recipients do not express hCD46.) (**F**) Percentage of human γ-globin$^+$ RBCs. Each symbol represents an individual animal.

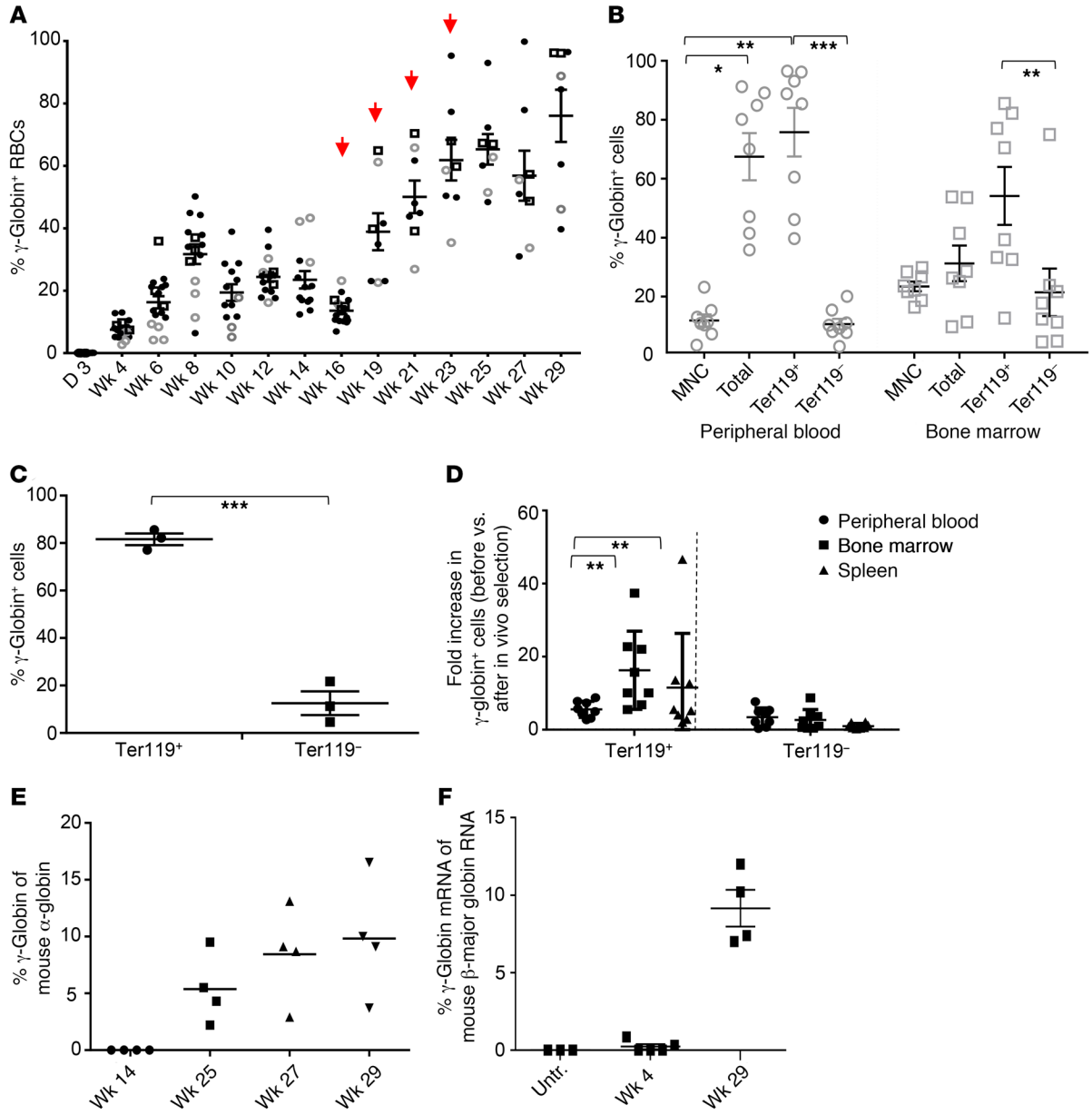

Figure 6. Analysis of γ-globin expression in in vivo–transduced CD46$^{+/+}$/Hbbth-3 mice after in vivo selection. (**A**) Percentage of human γ-globin in peripheral RBCs measured by flow cytometry. Red arrows indicate the time points of O^6-BG/BCNU treatment. Different symbols represent 3 independent experiments. The data up to week 16 are identical to those in Figure 5A. (**B**) Percentage of γ-globin–expressing cells in hematopoietic tissues at sacrifice (week 29) analyzed by flow cytometry. *$P \le 0.05$, **$P \le 0.0002$, ***$P \le 0.00003$. (**C**) γ-Globin expression in MACS-purified Ter119 cells. Bone marrow cells from primary recipients at week 29 were immunomagnetically selected for Ter119$^+$ cells. γ-Globin expression was measured in Ter119$^+$ and Ter119$^-$ cells by flow cytometry. ***$P \le 0.0002$. (**D**) Fold enrichment of γ-globin$^+$ erythroid (Ter119$^+$) and nonerythroid (Ter119$^-$) cells in peripheral blood, bone marrow, and spleen before versus after in vivo selection (week 16 vs. week 29). $n = 5$, **$P \le 0.0002$. (**E**) Percentage of human γ-globin protein compared with mouse α-globin protein, measured by HPLC in RBCs. Statistical analyses were done with the nonparametric Kruskal-Wallis test. (**F**) Level of human γ-globin mRNA over adult mouse β-major globin mRNA measured by RT-qPCR in peripheral blood cells. Untreated CD46$^{+/+}$/Hbbth-3 mice were used as control. Each symbol represents an individual animal.

after versus before in vivo selection (Figure 6D). However, the overall increase of γ-globin$^+$ marking in Ter119$^+$ cells in peripheral blood (where enucleated RBCs predominate) (Figure 6B) is probably due to the additive effect of the "natural" in vivo selection provided by the thalassemic background. The human γ-globin over mouse α-globin ratio in RBCs measured by HPLC increased from almost undetectable levels at week 14 to 10% at week 29 (Figure 6E and Supplemental Figure 8). Similarly, the level of γ-globin mRNA in blood cells of treated mice increased, translating into approximately 10% human γ-globin mRNA of mouse β-globin mRNA at week 29 (Figure 6F). In treated CD46$^{+/+}$/Hbbth-3 mice at week 29 after in vivo transduction, we measured approximately 1.5 γ-globin gene copies per cell (Supplemental Figure 9).

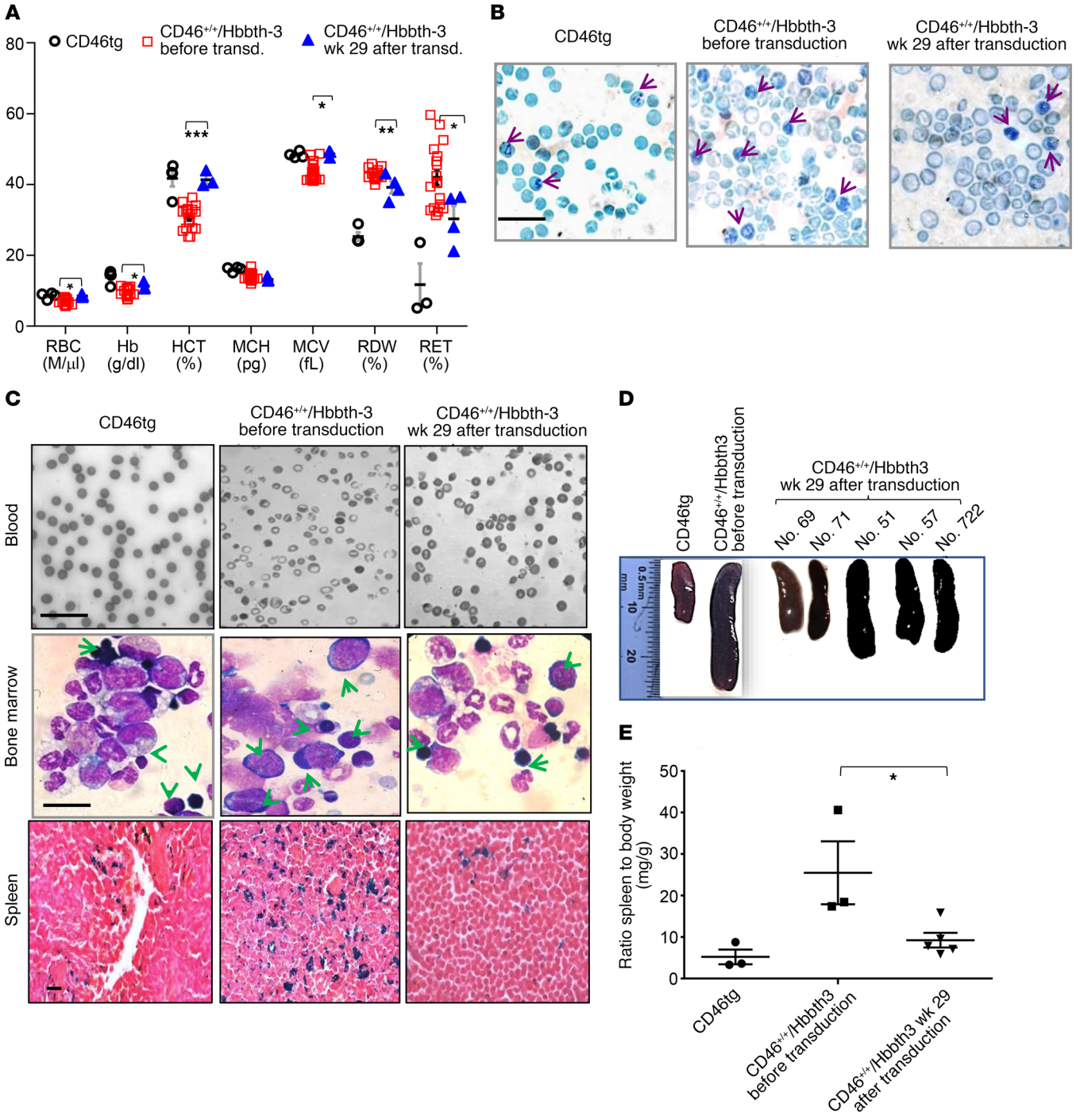

Figure 7. Phenotypic correction of CD46$^{+/+}$/Hbbth-3 mice by in vivo HSPC transduction/selection. (**A**) RBC analysis of healthy (CD46tg) mice, CD46$^{+/+}$/Hbbth-3 mice prior to mobilization and in vivo transduction, and CD46$^{+/+}$/Hbbth-3 mice that underwent in vivo transduction/selection (analyzed at week 29 after HDAd infusion) (n = 5). *$P \le 0.05$, **$P \le 0.0002$, ***$P \le 0.00003$. Statistical analysis was performed using 2-way ANOVA. (**B**) Supravital stain of peripheral blood smears with Brilliant cresyl blue for reticulocyte detection. Arrows indicate reticulocytes containing characteristic remnant RNA and micro-organelles. The percentages of positively stained reticulocytes in representative smears were: for CD46, 7%; for CD46$^{+/+}$/Hbbth-3 before treatment, 31%; and for CD46$^{+/+}$/Hbbth-3 after treatment, 12%. Scale bar: 20 μm. (**C**) Top: Blood smears. Scale bar: 20 μm. Middle: Bone marrow cytospins. Arrows indicate erythroblasts at different stages of maturation and a backshift in erythropoiesis with pro-erythroblast predominance in treated mice. Scale bar: 25 μm. Bottom: Tissue hemosiderosis by Perls' stain. Iron deposition is shown as cytoplasmic blue pigments of hemosiderin in spleen tissue sections. The blood smear images for the control mice (CD46tg and CD46$^{+/+}$/Hbbth-3, before transduction) in **C** and Figure 5D are from the same sample. (**D**) Macroscopic spleen images of 1 representative CD46tg and 1 untreated CD46$^{+/+}$/Hbbth-3 mouse and 5 treated CD46$^{+/+}$/Hbbth-3 mice. (**E**) At sacrifice, spleen size was determined as the ratio of spleen weight to total body weight (mg/g). Each symbol represents an individual animal. Data are presented as means ± SEM. *$P \le 0.05$. Statistical analysis was performed using 1-way ANOVA.

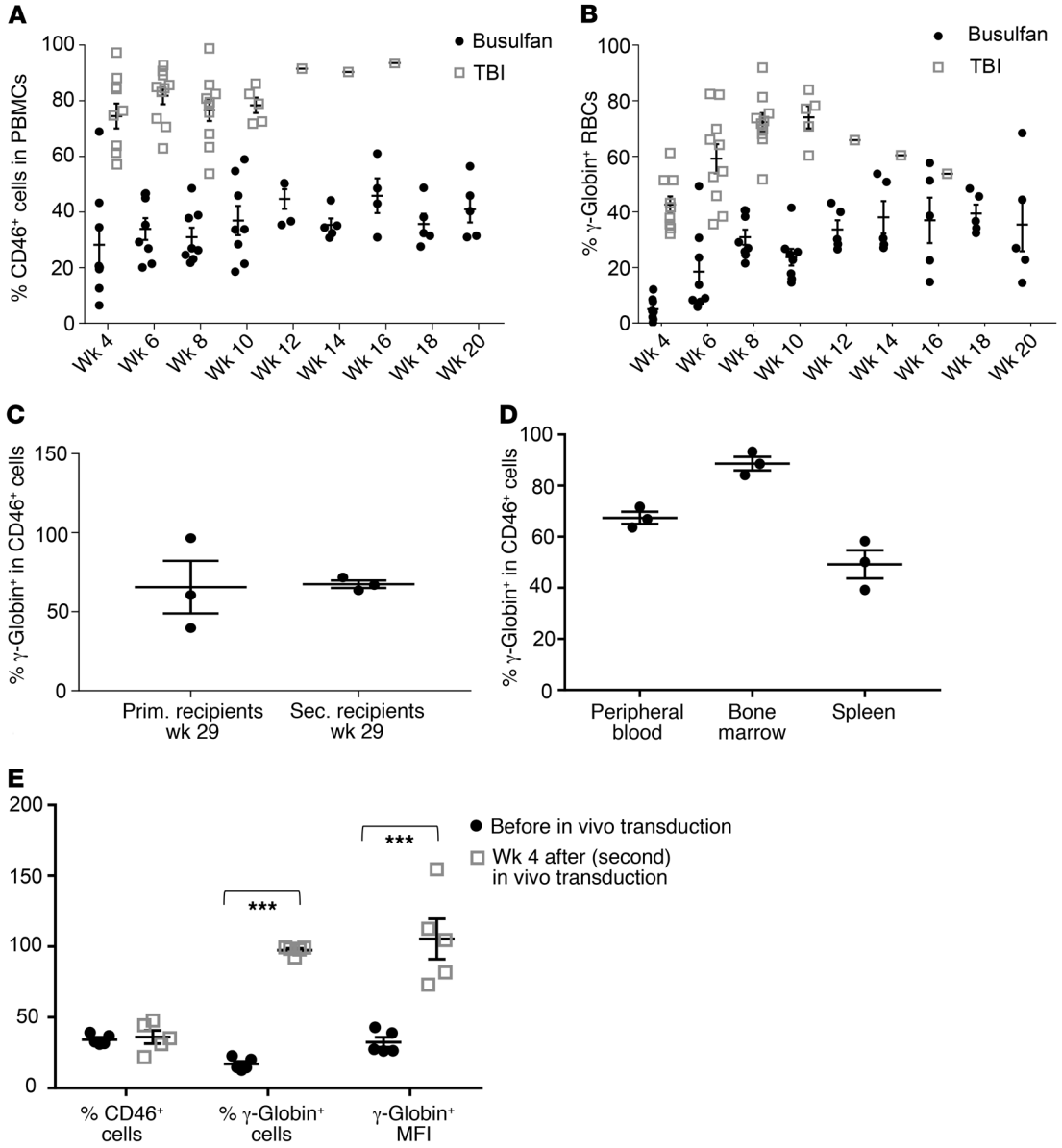

Figure 8. Analysis of secondary C57BL/6 recipients with transplanted bone marrow cells from treated CD46$^{+/+}$/Hbbth-3 mice. (**A**) Engraftment rates measured in the periphery based on the percentage of human CD46$^+$ (hCD46$^+$) cells in PBMCs after busulfan conditioning or total-body irradiation (TBI). (C57BL/6 recipients do not express hCD46.) (**B**) Percentage of human γ-globin–expressing peripheral blood RBCs. All mice received immunosuppression starting from week 4 after transplantation. (**C**) Percentage of γ-globin$^+$ cells in hCD46$^+$ (donor-derived) cells. (**C** and **D**) γ-Globin/CD46 expression in secondary C57BL/6 recipients at week 20 after transplant (busulfan preconditioning). CD46$^+$ cells were immunomagnetically separated from the chimeric bone marrow of 3 representative secondary mice and analyzed for γ-globin expression by flow cytometry. Notably, unlike humans, huCD46tg mice express CD46 on RBCs. (**C**) γ-Globin/CD46 marking rates of primary and secondary recipients at sacrifice. (**D**) γ-Globin expression in CD46$^+$-selected cells from the hematopoietic tissues of secondary recipients (week 20). Each symbol represents an individual animal. (**E**) γ-Globin expression in secondary recipients that received a new (second) round of HSPC mobilization/in vivo transduction (n = 5). Secondary recipients (busulfan-preconditioned) were analyzed for γ-globin and CD46 expression at week 20 after transplantation ("Before in vivo transduction"). These mice were then mobilized and transduced in vivo with the HDAd-γ-globin plus HDAd-SB vectors. Four weeks after in vivo transduction, mice were sacrificed and analyzed ("Week 4 after in vivo transduction"). ***$P \leq 0.00003$. Statistical analyses were performed using 1-way ANOVA.

Reversal of the thalassemic phenotype of CD46$^{+/+}$/Hbbth-3 mice after in vivo transduction/selection. Six weeks after the last dose of O^{6}BG/BCNU treatment, CD46$^{+/+}$/Hbbth-3 mice were sacrificed, and hematopoietic tissues were harvested for analysis. Hematological parameters at week 29 after in vivo transduction were significantly improved over baseline (Figure 7A) (RBCs: 8.53 ± 0.16 vs. 7.1 ± 0.13 M/μl, P = 0.01; hemoglobin: 11.27 ± 0.39 vs. 9.7 ± 0.18 g/dl, P = 0.05; hematocrit: 41.37% ± 0.81% vs. 30.7% ± 0.46%, P = 0.00001; mean corpuscular volume: 48.63 ± 0.36 vs. 43.5 ± 0.38 fl, P = 0.003; RBC distribution width: 39.5% ± 0.8% vs. 43% ± 0.3%, P = 0.006; reticulocytes: 31.13% ± 3.17% vs. 42.4% ± 1.43%, P = 0.05), and for specific red cell indices (hematocrit

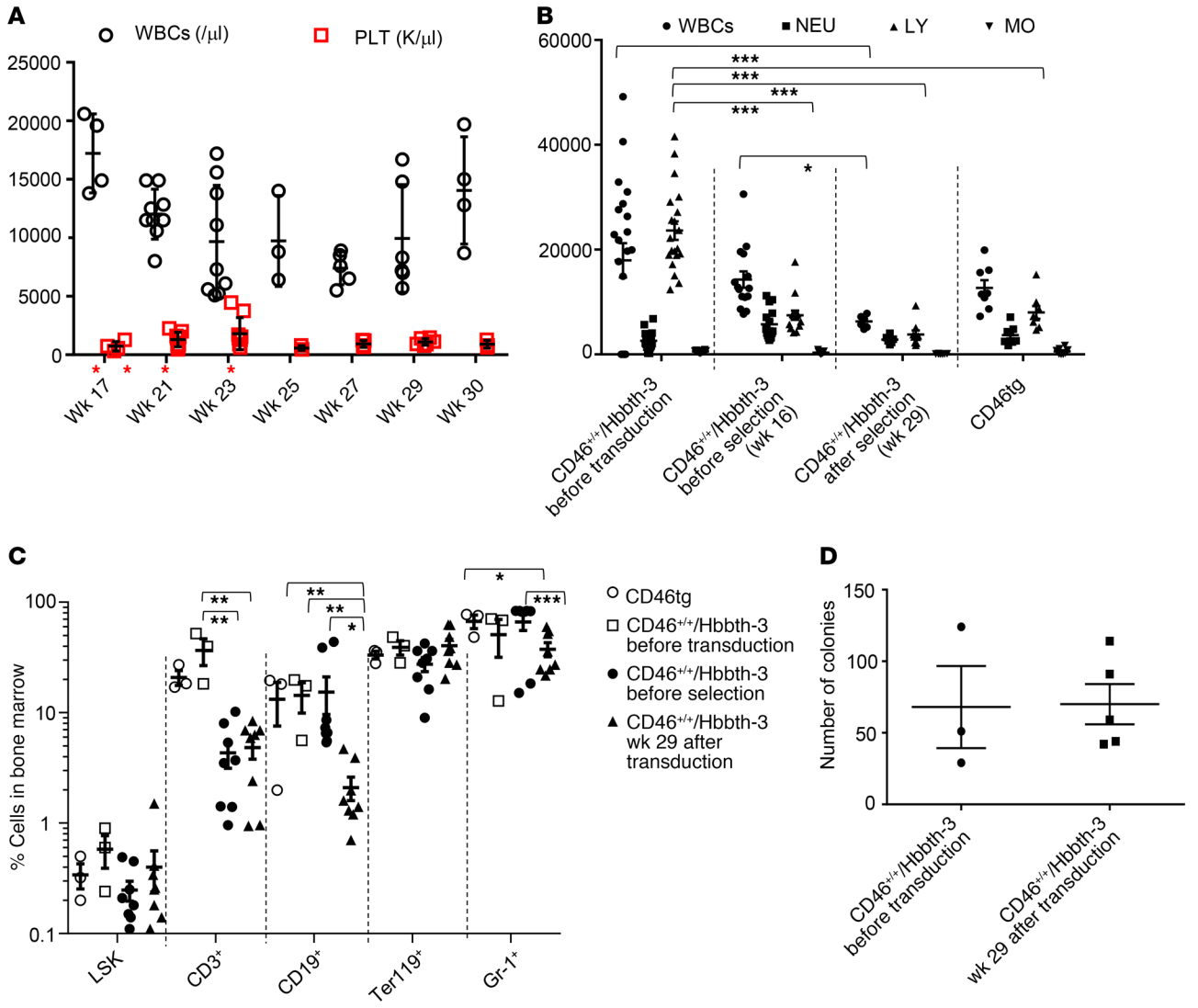

Figure 9. Safety of in vivo transduction/selection in the CD46$^{+/+}$/Hbbth-3 mouse model. (**A**) WBC and platelet (PLT) counts during and after in vivo selection. O^{6}BG/BCNU treatment is indicated by red asterisks. $n \geq 3$. (**B**) Absolute numbers of circulating WBC subpopulations. $n \geq 3$. (**C**) Cellular bone marrow composition in control and treated mice sacrificed at week 29. Shown is the percentage of lineage marker–positive cells (Ter119$^+$, CD3$^+$, CD19$^+$, and Gr-1$^+$ cells) and HSPCs (LSK cells). (**D**) Colony-forming potential of bone marrow cells harvested at week 29. Each symbol represents an individual animal. *$P \leq 0.05$, **$P \leq 0.0002$, ***$P \leq 0.00003$. Statistical analyses were performed using 2-way ANOVA. NEU: neutrophils; LY: lymphocytes; MO: monocytes.

[HCT], RBCs, mean corpuscular volume), levels were indistinguishable from their control CD46tg counterparts, suggesting near to complete phenotypic correction. Reticulocyte staining of blood smears demonstrated an impressive 3-fold reduction of reticulocyte numbers in treated CD46$^{+/+}$/Hbbth-3 mice with the highest percentage of γ-globin$^+$ RBCs (Figure 7B). Indicative of the reversal of the thalassemic phenotype in peripheral blood smears of the treated CD46$^{+/+}$/Hbbth-3 mice, the hypochromic, highly fragmented and anisopoikilocytic baseline RBCs were replaced by near-normochromic, well-shaped RBCs less variant in size (Figure 7C, top panels). In contrast to the blockade of erythroid lineage maturation in bone marrow of CD46$^{+/+}$/Hbbth-3 mice, represented by the prevalence of pro-erythroblasts and basophilic erythroblasts, in cytospins from control and treated CD46$^{+/+}$/Hbbth-3 mice, maturing erythroblasts predominated and were represented by polychromatic and orthochromatic erythroblasts (Figure 7C, middle panels). Intense parenchymal hemosiderosis was observed in the untreated CD46$^{+/+}$/Hbbth-3 mice, whereas only limited iron accumulation in the CD46tg and the treated CD46$^{+/+}$/Hbbth-3 mice could be detected (Figure 7C, bottom panels). Accordingly, spleen size, a measurable characteristic of compensatory hemopoiesis, was markedly reduced in treated animals (Figure 7, D and E).

In order to determine whether our combined in vivo transduction/selection approach resulted in genetic modification of primitive HSCs, bone marrow cells from treated CD46$^{+/+}$/Hbbth-3 mice harvested at week 29 (after transduction) were transplanted into C57BL/6 secondary recipients after either sublethal busulfan treatment or lethal total-body irradiation (TBI) (Figure 8, A and B). Although, as expected, the engraft-

ment rates in mice that received TBI were higher than those in busulfan-treated animals, the levels of expression adjusted to the engraftment levels did not show significantly different frequencies of γ-globin$^+$ RBCs. The fact that more than 75% of transplant-derived (CD46$^+$) erythrocytes were γ-globin$^+$ at week 20 after secondary transplantation and with a marking rate similar to that found in primary treated mice at week 29 (Figure 8, C and D) under the competitive conditions generated by the submyeloablative busulfan conditioning in a normal recipient background (in which the HDAd-γ-globin/HDAd-SB–transduced CD46$^{+/+}$/Hbbth-3 HSPCs had no selective advantage) further supports the conclusion that our approach results in the genetic correction of long-term repopulating HSCs. Moreover, secondary, busulfan-conditioned C57BL/6 recipients at week 20 after transplant that were submitted to mobilization and in vivo transduction demonstrated a remarkable enrichment in γ-globin–expressing cells and a significant increase in expression/MFI (Figure 8E).

Safety of in vivo HSPC transduction with HDAd-γ-globin/mgmt plus HDAd-SB followed by O^6-BG/BCNU in vivo selection. In our mouse studies, the procedure was well tolerated. No overt hematological abnormalities were observed. At time of sacrifice, 6 weeks after the last O^{6}GB/BCNU dose, all hematological values were within normal ranges, although the total WBC counts were lower compared with levels before in vivo selection, suggesting a cytoreductive effect of drug treatment on WBCs — in particular, lymphocytes (Figure 9, A and B). This effect was also reflected in the reduced frequency of CD3$^+$, CD19$^+$, and Gr-1$^+$ cells in bone marrow as compared with their untreated or preselection counterparts (Figure 9C). Notably, even at their nadir (week 25–27; 2–4 weeks after the last O^{6}BG/BCNU injection), the WBCs and platelets never reached aplasia levels (i.e., neutrophils <1,000/μl, platelets <20,000/μl), and the WBCs started to recover by week 30 (7 weeks after the last O^{6}BG/BCNU injection). This together with our observation that in the CD46tg model, WBCs and lymphocyte counts returned to pretreatment levels 10 weeks after the last O^{6}BG/BCNU injection (Figure 3A), suggests that the cytoreductive effect of the in vivo selection drugs is mild and transient. Importantly, the bone marrow cell composition in the percentage of LSK and Ter119$^+$ cells, as well as the colony-forming potential of bone marrow cells, was not affected by the in vivo transduction/selection of HSPCs (Figure 9, C and D).

Discussion

Despite the unequivocal clinical progress in ex vivo HSPC gene therapy of hemoglobinopathies, the need for myeloablative conditioning in order to reach clinically relevant HSPC engraftment rates is a major limitation. Furthermore, the technical complexity allows the implementation of such treatment in only a small number of specialized and/or accredited centers. We developed an in vivo HSPC gene therapy approach that does not require myeloablation and HSPC cell transplantation and therefore has the potential to make HSPC gene therapy for thalassemia safer and more accessible. The central idea of our approach is to mobilize HSPCs from the bone marrow and, while they circulate at high numbers in the periphery, transduce them with an intravenously injected HSPC-tropic HDAd5/35++ gene transfer vector system. The novel features of the HDAd5/35++ vector system include (a) CD46-affinity-enhanced fibers that allow for efficient transduction of primitive HSCs while avoiding infection of nonhematopoietic tissues after intravenous injection, (b) an SB100X transposase–based integration system that functions independently of cellular factors and mediates random transgene integration without a preference for genes, and (c) an MGMT(P140K) expression cassette mediating selective survival and expansion of progeny cells without affecting the pool of transduced primitive HSCs by short-term treatment with low-dose O^{6}BG/BCNU (13). Additional features that distinguish HDAd5/35++ vectors from currently used SIN-lentiviral (SIN-LV) vectors include their large (30 kb) insert capacity, which, in this study, was used to incorporate a micro-LCR/β-promoter–driven γ-globin gene and an EF1A promoter–driven *MGMT(P140K)* gene with a size of 11.8 kb. Furthermore, the production of HDAd5/35++ vectors does not require large-scale plasmid transfections and yields more than 3×10^{12} infectious particles per liter spinner culture. Notably, the yields of SIN-LV vectors used in clinical trials for hemoglobinopathies are at least 2 orders of magnitude lower.

Efficacy of the in vivo approach. In contrast to HSPC gene therapy of other genetic diseases (i.e., X-linked SCID, ref. 19; ADA-SCID, ref. 20; or Wiskott-Aldrich syndrome, ref. 21) where stable transduction of less than 1% of HSPCs provides a significant clinical benefit, phenotypic correction of hemoglobinopathies in patients requires at least 20% corrected erythroid precursors (22–24). In murine models for hemoglobinopathies, γ-globin expression at about 15% of the total α-globin mRNA was sufficient for therapy (22, 25, 26). In our study, after in vivo transduction/selection, more than 60% of bone marrow erythroblasts expressed γ-globin in the in vivo transduced CD46tg and CD46$^{+/+}$/Hbbth-3 models (Figure 1C and Figure 6A). This translated into 40%–97% circulating γ-globin–expressing RBCs (Figure 1D and Figure 6B). Importantly also, in both animal models, sustained γ-globin marking in RBCs was demonstrated in secondary recipients, suggesting that primitive, long-term repopulating HSCs were initially transduced by our vector system.

Our qPCR studies detected 2 to 3 integrated transgene copies per cell in the overwhelming majority of bone marrow cells. In agreement with earlier studies (18, 27), we did not find that vivo selection selected for high-copy-number clones. Taking into account our genome-wide integration site analysis, we project approximately 1,000 originally transduced HSCs. Considering that mice have 10,000 to 20,000 HSCs (28, 29), this would mean that our vector system targeted approximately 5%–10% of HSCs, which would be a solid basis for a polyclonal reconstitution of hematopoiesis after in vivo selection and for a long-term therapeutic effect.

In the thalassemia intermedia model, a near-complete phenotypic correction was achieved. Key hematological parameters (HCTs, RBCs, mean corpuscular volume) were indistinguishable from their counterparts in "healthy" (parental CD46tg) mice. The degree of correction of RBC indices and morphology correlated with the level of γ-globin–expressing cells in individual mice. Peripheral RBCs and erythroid bone marrow precursor cells resembled those of healthy mice in both morphology and the maturation process. Extramedullary hematopoiesis and parenchy-

mal iron deposition regressed, and spleen size was significantly reduced. The thalassemic phenotype in the CD46$^{+/+}$/Hbbth-3 model was also characterized by leukocytosis/lymphocytosis (Supplemental Figure 5). (Leukocytosis/lymphocytosis is also often present in splenectomized thalassemia/sickle cell disease patients or patients with functional, disease-associated asplenia; ref. 30.) Interestingly, WBC counts in CD46++/Hbbth-3 mice returned to levels of "healthy" CD46tg mice at week 29 after in vivo transduction (Figure 9A). This effect suggests that the reversal of the thalassemic phenotype by our approach extends beyond the erythroid compartment, resulting in normalization of WBCs, and most likely overall spleen function.

Notably, in contrast to the study in CD46tg mice, in the context of a thalassemic background and in the absence of O^{6}BG/BCNU treatment, 13% of γ-globin$^+$ RBCs were circulating in peripheral blood of CD46$^{+/+}$/Hbbth-3 mice, and this level was maintained long-term in secondary recipients. This indicates that γ-globin gene expression conferred a survival advantage to thalassemic genetically modified erythroid precursors similar to what was reported with ex vivo lentivector HSPC gene therapy in a mouse model of thalassemia major (17). However, the phenotypic correction in the thalassemia mouse model required O^{6}BG/BCNU treatment. This suggests that, if required because of low globin marking, the inducible in vivo selection system allows for salvaging of the therapeutic efficacy by an easy pharmacological intervention.

Although some treated CD46$^{+/+}$/Hbbth-3 mice had nearly 100% γ-globin$^+$ RBCs, the level of γ-globin expression was only 10%–15% of that of adult mouse globin. Notably, a similar discrepancy was reported by Zhao et al. using a micro-LCR/γ-globin/mgmt cassette in the context of a lentivirus vector (18). While our in vivo approach showed promising therapeutic efficacy in a model for thalassemia intermedia, the cure of patients with β0/β0 thalassemia or β+/β+ genotypes with lower levels of overall hemoglobin output would, most likely, require higher γ-globin levels than achieved with our current HDAd-γ-globin/mgmt vector. The relatively low number of integrated γ-globin transgenes (2–3 per HSC/CFU) as well as a suboptimal activity of the micro–(HS1–HS4) β-globin LCR in mouse cells could account for this relatively low expression level. To increase the level of γ-globin in murine thalassemia models, we consider the following possibilities: (a) The ratio of HDAd-SB to HDAd-γ-globin/mgmt vectors could be changed from 1:1 to 1:3 to increase the number of integrated transgene copies per cell (31). (b) We are also planning to use a 26.1-kb version of β-globin LCR to drive γ-globin expression to minimize transgene integration position effects (32). (c) In addition to the SB100X-based γ-globin gene addition system, our HDAd5/35++ vector could accommodate a CRISPR/Cas9 to disrupt γ-globin suppressor regions and reactivate the endogenous γ-globin genes (33). A second round of mobilization and HDAd injection (4 weeks after the first round) did not result in transduction of peripheral blood cells because of the development of neutralizing serum antibodies against the virus (Supplemental Figure 10). However, as our in vivo transduction studies in secondary transplant recipients indicate (Figure 8E), if the development of anti-HDAd antibodies could be pharmaceutically blocked, a second treatment could increase both the percentage of γ-globin$^+$ RBCs and the γ-globin expression level/MFI.

The CD46$^{+/+}$/Hbbth-3 model for thalassemia intermedia served here, as a proof of principle, to demonstrate the potential of our in vivo approach to treat thalassemia. Clearly, the clinical target for such an approach would be patients with thalassemia major. Studies using the homozygous Hbbth-3 mouse model of lethal thalassemia major are complicated by the fact that human γ-globin is strongly prone to form possibly deleterious γ4 homotetramers in transgenic mice due to a relative inefficiency of hybrid mouse α-globin/human γ-globin heterotetramer formation (34). Even high-level expression of human γ-globin (27% of mouse α-globin) could only prolong but not support survival of homozygous Hbbth-3 mice (35). In contrast, thalassemia major patients with hereditary persistence of fetal hemoglobin (HbF) could survive at such an HbF level (36). Therefore, only the heterozygous Hbbth-3 model of thalassemia intermedia can be reliably used for the preclinical assessment of γ-globin gene therapy approaches.

Safety of the in vivo HSPC transduction/selection approach. Our approach abrogates the need for myeloablation/conditioning and its associated toxicity, while it has the capability to effectively target HSPCs in the unconditioned host by simple intravenous and subcutaneous substance/vector injections. Importantly, the procedure has been well tolerated in all animals involved in this study.

Concerning the HSPC mobilization based on G-CSF/AMD3100 (plerixafor), the approach has been clinically proven safe and efficacious and is routinely used for HSPC mobilization and collection by leukapheresis in all running trials for thalassemia major (2, 37). As an alternative to the mobilization regimen used in this study, we are currently testing approaches that involve the continuous blockade of CXCR4 by small synthetic molecules to achieve a more efficient mobilization of HSPCs (38).

The intravenous injection of HDAd5/35++ vectors does not result in transgene expression in tissues other than the mobilized HSPCs and PBMCs in CD46tg mice at day 3 after injection (6). This was in agreement with our early studies in baboons with intravenously injected first-generation CD46-targeting Ad5/35 and Ad5/11 vectors (39). A potential explanation for this tropism is that CD46 receptor density and accessibility are not sufficiently high in nonhematopoietic tissues to allow for efficient viral transduction (6, 40). Here, we measured the number of integrated transgene copies per cell in different tissues at week 18 after in vivo transduction/selection (Supplemental Figure 11). The copy number in bone marrow, PBMCs, and spleen was around 2.5. Integrated transgenes were also detected in the genomic DNA from liver, lung, and intestine. Previous studies with a GFP vector system have shown that the signals in these organs originate from infiltrating blood cells and/or residential macrophages (6).

Intravenous injection of HDAd vectors (but also other viral vectors) is associated with the release of proinflammatory cytokines (41, 42), which can, however, efficiently be blocked by pretreatment with glucocorticoids the day before virus injection (43)

or vector dose fractionation (44). Good safety profiles of intravenously injected oncolytic adenoviruses have been documented in dozens of clinical trials, including a trial with a CD46-targeting oncolytic adenovirus (45).

Regarding the safety of in vivo selection and the concern that O^6BG/BCNU–stimulated proliferation may deplete the reservoir of long-term quiescent HSPCs, studies with large-animal models have provided evidence for long-term multilineage selection without HSPC exhaustion or emergence of dominant clones (10, 46). In these models, the hematopoietic and the extramedullary toxicity profile was acceptable. In the present study and our previous mouse studies (13, 47), in vivo selection was well tolerated without myelosuppression. No changes in the frequency of bone marrow HSPCs upon O^6BG/BCNU treatment were observed. A mild decrease in WBCs, specifically lymphocyte counts, was transient. Three to four cycles of low-dose treatment with O^6BG, an inhibitor of DNA repair processes, and BCNU, an alkylating agent, resulting in survival of in vivo selected HSPCs could, theoretically, trigger mutations and tumorigenesis. Arguing against this risk are long-term follow-up studies in monkeys and dogs that received such treatment and did not suggest signs of carcinogenesis (10, 48, 49). In an attempt to assess this risk in HSPCs, we performed an in vitro study with $CD34^+$ cells transduced with an MGMT (P140K)-expressing HDAd vector and subjected to O^6BG/BCNU treatment at a dose that killed 98% of cells that were not protected by MGMT(P140K) expression (Supplemental Figure 12, A–C). At day 14 after drug exposure, we performed Illumina whole exome sequencing of $CD34^+$ cells without treatment and cells that survived the treatment (Supplemental Figure 13, A and B). Using Sorting Intolerant from Tolerant (SIFT; https://www.uswest.ensemble.org) as a filter that predicts whether an amino acid substitution affects protein function, we identified 126 de novo mutations per 47,858,908 sequenced base pairs in the treated sample (2.63×10^{-6} mutations per base pair) (Supplemental Table 1) Using ClinVar as a filter, we found 6 mutations with potential pathological effects. The finding that O^6BG/BCNU treatment causes mutations is not unexpected; however, the consequences of our exome sequencing data are unclear. Loss-of-function variants are common in the human population. A recent analysis by the Exome Aggregation Consortium identified 3,230 genes with loss-of-function mutations, with 72% of these variants having no currently established human disease phenotype (50).

The HDAd-SB vector that carries SB100X transposase and Flpe recombinases gene does not integrate and is lost during cell division (51). In agreement with our previously published data (51), neither integrated nor episomal HDAd-SB vector was detectable by qPCR at the end of the studies in bone marrow Lin^- cells. We and others previously documented that SB100X transposase mediates random transgene integration without a preference for integration into or near genes (6, 31). Here, we show that this random pattern is maintained after in vivo selection without the emergence of dominant integration sites/clones. Theoretically, random integration is relatively safer than preferential integration into active genes, which occurs during lentivirus or AAV vector transduction (52–54). Notably, in a SIN-LV–based clinical trial for β-thalassemia, integration into an intron of the *HMGA2* proto-oncogene triggered a benign clonal dominance in one patient (3).

To reduce the risk of potential tumorigenicity from a combined effect of SB100X-mediated random transgene integration and treatment with mutagenic selection drugs, we have developed a vector system that would eliminate the first risk factor. It mediated targeted γ-globin integration into a chromosomal safe harbor site and resulted in stable γ-globin marking in more than 70% of RBCs in mice (55).

Undoubtedly, the safety of our approach has to be first clearly documented in stringent long-term studies in nonhuman primates. In this context it is notable that macaque and baboon bone marrow $CD34^+$ cells are as efficiently transduced by Ad5/35 vectors as human $CD34^+$ cells (56), and we recently demonstrated direct in vivo transduction of mobilized $CD34^+$ cells by an integrating HDAd5/35++ vector expressing GFP in macaques (57).

Toward the clinical translation of our approach. Production of HDAd5/35++ vectors routinely yields approximately 5×10^{12} viral particles (vp) per liter spinner culture. cGMP-grade HDAd production for Flexion's FX201 vector is established. Protocols for the pharmacological control of innate immune reaction to intravenously injected virus are more developed for humans than for mice and are currently practiced in clinical trials with intravenously injected high-dose rAAV vectors. However, the majority of humans have neutralizing serum antibodies directed against Ad5 capsid proteins, which will block in vivo transduction with HDAd5/35 vectors, i.e., vectors that contain Ad5 capsid proteins and chimeric Ad35 fibers. An alternative would be vectors derived from Ad35. Ad35 is one of the rarest of the 57 known human serotypes, with a seroprevalence of less than 7% and no cross-reactivity with Ad5 (58–62). Ad35 is less immunogenic than Ad5 (63), which is, in part, due to attenuation of T cell activation by the Ad35 fiber knob (64–66). After intravenous injection, there is only minimal transduction (only detectable by PCR) of tissues, including the liver, in human CD46–transgenic mice (67) and nonhuman primates (68). First-generation Ad35 vectors have been used clinically for vaccination purposes (69, 70). For potential studies in humans, we will therefore generate vectors based on HDAd35++ for in vivo HSPC gene therapy.

In summary, we propose here an alternative to traditional lentivirus vector ex vivo gene therapy for thalassemia, which we expect to simplify the therapy and, theoretically, make it accessible to resource-poor regions where thalassemia major is endemic and HSPC transplantation not feasible.

Methods

Reagents. The following reagents were used: G-CSF (Neupogen, Amgen), AMD3100 (Sigma-Aldrich), plerixafor (Mozobil, Genzyme Corp.), O^6-BG and BCNU (Sigma-Aldrich), mycophenolate mofetil (CellCept Intravenous, Genentech), rapamycin (Rapamune/Sirolimus, Pfizer), and methylprednisolone (Pfizer).

HDAd vectors. The generation of the transposon vector HDAd-γ-globin/mgmt and the SB100X-expressing human embryonic kidney-293 cell-derived 116 cells (71) has been described previously (51). Helper virus contamination levels were found to be less than

0.05%. Titers were 6×10^{12} to 12×10^{12} vp/ml. All HDAd vectors used in this study contain chimeric fibers composed of the Ad5 fiber tail, the Ad35 fiber shaft, and the affinity-enhanced Ad35++ fiber knob (72). All of our HDAd preparations had less than 1 copy wild-type virus in 10^{10} vp (measured by qPCR using the primers described elsewhere; ref. 73).

Intracellular flow cytometry detecting human γ-globin expression. The FIX and PERM cell permeabilization kit (Thermo Fisher Scientific) was used, and the manufacturer's protocol was followed. Briefly, approximately 1×10^6 cells were resuspended in 100 μl FACS buffer (PBS supplemented with 1% FCS), 100 μl reagent A (fixation medium) was added and incubated for 2–3 minutes at room temperature, and 1 ml precooled absolute methanol was then added, mixed, and incubated on ice in the dark for 10 minutes. The samples were then washed with FACS buffer and resuspended in 100 μl reagent B (permeabilization medium) and 1 μg γ-globin antibody (Santa Cruz Biotechnology, catalog sc-21756 PE), incubated for 30 minutes at room temperature. After the wash, cells were resuspended in FACS buffer and analyzed. For erythroid and γ-globin double staining, cells were stained with APC anti–mouse Ter119 antibody (Ter119-APC, BioLegend, catalog 116212) first, and then washed and fixed with fixation medium as described above.

Globin HPLC. Individual globin chain levels were quantified on a Shimadzu Prominence instrument with an SPD-10AV diode array detector and an LC-10AT binary pump (Shimadzu). A 38%–60% gradient mixture of 0.1% trifluoroacetic acid in water/acetonitrile was applied at a rate of 1 ml/min using a Vydac C4 reversed-phase column (Hichrom).

Real-time reverse transcription PCR. Total RNA was extracted from 50–100 μl blood using Trizol reagent (Thermo Fisher Scientific, catalog 15596026) following the manufacturer's phenol-chloroform extraction method. QuantiTect reverse transcription kit (Qiagen, catalog 205311) and Power SYBR Green PCR Master Mix (Thermo Fisher Scientific, catalog 4367659) were used. Real-time quantitative PCR was performed on a StepOnePlus Real-Time PCR System (Applied Biosystems). The following primer pairs were used in this work: mouse RPL10 forward, 5′-TGAAGACATGGTTGCTGAGAAG-3′, and reverse, 5′-GAACGATTTGGTAGGGTATAGGAG-3′; human γ-globin forward, 5′-GTGGAAGATGCTGGAGGAGAAA-3′, and reverse, 5′-TGCCATGTGCCTTGACTTTG-3′; mouse β-major globin forward, 5′-ATGCCAAAGTGAAGGCCCAT-3′, and reverse, 5′-CCCAGCACAATCACGATCAT-3′.

Magnetic cell sorting. For the depletion of lineage-committed cells, the mouse Lineage Cell Depletion Kit (Miltenyi Biotec, catalog 130-090-858) was used according to the manufacturer's instructions. For the selection of Ter119$^+$ cells from the bone marrow of primary CD46$^{+/+}$/Hbbth-3 mice or CD46$^+$ cells from the hematopoietic tissues of secondary C57BL/6 recipients, mouse anti-Ter119 microbeads (Miltenyi Biotec, catalog 130-049-901) or anti-PE microbeads (Miltenyi Biotec, catalog 130-048-801) following staining with human anti–CD46-PE primary antibody (Miltenyi Biotec, catalog 130-104-508) were used, respectively.

Animal studies. C57BL/6-based transgenic mice that are homozygous for the human CD46 genomic locus (CD46tg) and provide CD46 expression at a level and in a pattern similar to that in humans were described earlier (14). CD46tg mice were provided by Roberto Cattaneo, Mayo Clinic (Rochester, Minnesota, USA). A thalassemic mouse model susceptible to infection by HDAd5/35++ vectors was obtained by breeding of female CD46tg mice with male Hbbth-3 mice (The Jackson Laboratory) and backcrossing of F_1 with CD46tg mice, to generate CD46$^{+/+}$/Hbbth-3 mice. Six- to ten-week-old female CD46tg and CD46$^{+/+}$/Hbbth-3 females were used for the in vivo transduction/selection studies. Six- to ten-week-old female C57BL/6 mice were used as secondary recipients.

Mobilization and in vivo transduction of CD46tg mice. HSPCs were mobilized in mice by s.c. injections of human recombinant G-CSF (5 μg/mouse per day, 4 days) followed by an s.c. injection of AMD3100 (5 mg/kg) on day 5. In addition, animals received dexamethasone (10 mg/kg) i.p. 16 and 2 hours before virus injection. Thirty and 60 minutes after AMD3100, animals were injected i.v. with HDAd-γ-globin/mgmt plus HDAd-SB through the retro-orbital plexus with a dose of 4×10^{10} vp per injection (total 2 injections, 30 minutes apart). Four weeks later, mice were injected with O^6-BG (15 mg/kg, i.p.) 2 times, 30 minutes apart. One hour after the second injection of O^6-BG, mice were injected with BCNU (5 mg/kg, i.p.). The BCNU dose was increased in the second and third cycles to 7.5 and 10 mg/kg, respectively.

Mobilization and in vivo transduction of CD46$^{+/+}$/ Hbbth-3 mice. In these studies, a 7-day mobilization approach with G-CSF 250 μg/kg i.p. (1–6 days) and plerixafor 5 mg/kg i.p. (formerly AMD3100; Mozobil, Genzyme Corp.) (days 5–7) was applied, as previously described in a thalassemic mouse model (16). In vivo transduction was performed as above. Following treatment, combined immunosuppression was administered. At week 17, mice were subjected to 4 cycles of in vivo selection with O^{6}BG (30 mg/kg, i.p.) and escalated BCNU doses (5, 7.5, 10, 10 mg/kg) with a 2-week interval between doses. Immunosuppression was resumed 2 weeks after the last O^6-BG/BCNU dose.

Immunosuppression. Daily i.p. injection of mycophenolate mofetil (20 mg/kg/d), rapamycin (0.2 mg/kg/d), and methylprednisolone (20 mg/kg/d) was performed.

Secondary bone marrow transplantation. Recipients were female C57BL/6 mice, 6–8 weeks old, from The Jackson Laboratory. On the day of transplantation, recipient mice were irradiated with 10 Gy. Bone marrow cells from in vivo–transduced CD46tg mice were isolated aseptically, and lineage-depleted cells were isolated using magnetic cell sorting (MACS). Four hours after irradiation, cells were injected i.v. at 1×10^6 cells per mouse. In the CD46$^{+/+}$/Hbbth-3 mouse studies, 2×10^6 whole bone marrow cells from in vivo–transduced CD46$^{+/+}$/Hbbth-3 mice were transplanted into submyeloablated secondary C57BL/6 recipients conditioned with 100 mg/kg i.p. busulfan (Busilvex, Pierre Fabre) divided into 3 daily doses or lethal TBI (1,000 cGy). At week 20, secondary recipients were sacrificed, and CD46$^+$ cells from blood, bone marrow, and spleen were either isolated by MACS, or mice were subjected to mobilization and in vivo transduction, as described above. All secondary recipients received immunosuppression starting at week 4.

Tissue analysis. Spleen and liver tissue sections of 2.5 μm thickness were fixed in 4% formaldehyde for at least 24 hours, dehydrated, and embedded in paraffin. Staining with H&E was used for histological evaluation of extramedullary hemopoiesis. Hemosiderin was detected in tissue sections by Perls' Prussian blue staining. Briefly, the tissue sections were treated with a mixture of equal volumes (2%) of potassium ferrocyanide and hydrochloric acid in distilled water and then counterstained with neutral red. The spleen size was assessed as the ratio of spleen weight (mg) to body weight (g).

Blood analysis and bone marrow cytospins. Blood samples were collected into EDTA-coated tubes, and analysis was performed on a HemaVet 950FS (Drew Scientific) or ProCyteDx (IDEXX) machine. Peripheral blood smears were prepared and stained with May-Grünwald/Giemsa for 5 and 15 minutes, respectively (Merck). Suspensions of bone marrow cells were centrifuged onto slides using a cytospin device and stained with May-Grünwald/Giemsa.

The following methods are described in the Supplemental Methods online: flow cytometry of cell surface markers, colony-forming unit assays, integration site analysis by LAM-PCR/next-generation sequencing, vector genome biodistribution by qPCR, vector copy number per single cell by qPCR, next-generation exome sequencing, and anti-adenovirus serum IgG antibody titers by ELISA.

Statistics. Data are presented as means ± SEM. For comparisons of multiple groups, 1-way and 2-way ANOVA with Bonferroni post-testing for multiple comparisons was used. Differences between groups for 1 grouping variable were determined by unpaired, 2-tailed Student's *t* test. For nonparametric analyses, the Kruskal-Wallis test was used. Statistical analysis was performed using GraphPad Prism version 6.01 (GraphPad Software Inc.). A *P* value less than 0.05 was considered significant; $^{*}P \leq 0.05$, $^{**}P \leq 0.0002$, $^{***}P \leq 0.00003$.

Animal study approval. All experiments involving animals were conducted in accordance with the institutional guidelines set forth by the University of Washington. The University of Washington is an Association for the Assessment and Accreditation of Laboratory Animal Care International (AAALAC)–accredited research institution, and all live animal work conducted at this university is in accordance with the Office of Laboratory Animal Welfare Public Health Assurance policy, the US Department of Agriculture Animal Welfare Act and Regulations, the Guide for the Care and Use of Laboratory Animals (National Academies Press, 2011), and the University of Washington's Institutional Animal Care and Use Committee (IACUC) policies. The studies were approved by the IACUC of the University of Washington (protocol 3108-01) and the George Papanicolaou Hospital (protocol 477957/4580).

Author contributions

AL provided the conceptual framework for the study. AL and EY designed the experiments. EY supervised the studies in thalassemia mice. HW, AG, NP, CL, HBS, EY, and AL performed the experiments. AE provided critical material. CC, AA, ZI, and TP provided critical comments on the manuscript. AL and EY wrote the manuscript.

Acknowledgments

The study was supported by NIH grants R21CA193077 and R01HL128288, a grant from the Wings of Karen Foundation, and a grant from the Marsha Rivkin Foundation (to AL). NP was supported by the Cooley's Anemia Foundation. AG was supported by a scholarship from the Foundation of the Hellenic Society of Hematology. We thank Sucheol Gil for technical support. We thank Hans-Peter Kiem and Jennifer Adair (Fred Hutchinson Cancer Research Center) for helpful discussions about the in vivo selection system. This paper is dedicated to the late George Stamatoyannopoulos.

Address correspondence to: Evangelia Yannaki, Gene and Cell Therapy Center, Hematology Department, HCT Unit, George Papanicolaou Hospital, Thessaloniki 57010, Greece. Phone: 30.2313.307518; Email: eyannaki@u.washington.edu. Or to: André Lieber, University of Washington, Department of Medicine, Division of Medical Genetics, Box 357720, Seattle, Washington 98195, USA. Phone: 206.221.3973; Email: lieber00@uw.edu.

1. Weatherall DJ. Thalassemia as a global health problem: recent progress toward its control in the developing countries. *Ann N Y Acad Sci*. 2010;1202:17–23.
2. Psatha N, Papayanni PG, Yannaki E. A new era for hemoglobinopathies: more than one curative option. *Curr Gene Ther*. 2017;17(5):364–378.
3. Cavazzana-Calvo M, et al. Transfusion independence and HMGA2 activation after gene therapy of human β-thalassaemia. *Nature*. 2010;467(7313):318–322.
4. Ferrari G, Cacazzana M, Mavilio F. Gene therapy approaches to hemoglobinopathies. In: Bauer DE, Kohn DB, eds. *Hematology/Oncology Clinics of North America: Gene Therapy*. Vol. 31. Issue 5. Philadelphia, Pennsylvania, USA: Elsevier; 2017:835–852.
5. Thompson AA, et al. Gene therapy in patients with transfusion-dependent β-thalassemia. *N Engl J Med*. 2018;378(16):1479–1493.
6. Richter M, et al. In vivo transduction of primitive mobilized hematopoietic stem cells after intravenous injection of integrating adenovirus vectors. *Blood*. 2016;128(18):2206–2217.
7. Richter M, et al. In vivo hematopoietic stem cell transduction. *Hematol Oncol Clin North Am*. 2017;31(5):771–785.
8. Ren J, Stroncek DF. Gene therapy simplified. *Blood*. 2016;128(18):2194–2195.
9. Mátés L, et al. Molecular evolution of a novel hyperactive Sleeping Beauty transposase enables robust stable gene transfer in vertebrates. *Nat Genet*. 2009;41(6):753–761.
10. Beard BC, Trobridge GD, Ironside C, McCune JS, Adair JE, Kiem HP. Efficient and stable MGMT-mediated selection of long-term repopulating stem cells in nonhuman primates. *J Clin Invest*. 2010;120(7):2345–2354.
11. Larochelle A, et al. In vivo selection of hematopoietic progenitor cells and temozolomide dose intensification in rhesus macaques through lentiviral transduction with a drug resistance gene. *J Clin Invest*. 2009;119(7):1952–1963.
12. Trobridge GD, Beard BC, Wu RA, Ironside C, Malik P, Kiem HP. Stem cell selection in vivo using foamy vectors cures canine pyruvate kinase deficiency. *PLoS One*. 2012;7(9):e45173.
13. Wang H, et al. A combined in vivo HSC transduction/selection approach results in efficient and stable gene expression in peripheral blood cells in mice. *Mol Ther Methods Clin Dev*. 2018;8:52–64.
14. Kemper C, et al. Membrane cofactor protein (MCP; CD46) expression in transgenic mice. *Clin Exp Immunol*. 2001;124(2):180–189.
15. Yang B, Kirby S, Lewis J, Detloff PJ, Maeda N, Smithies O. A mouse model for β0-thalassemia. *Proc Natl Acad Sci U S A*. 1995;92(25):11608–11612.
16. Psatha N, et al. Superior long-term repopulating capacity of G-CSF+plerixafor-mobilized blood: implications for stem cell gene therapy by studies in the Hbb(th-3) mouse model. *Hum Gene Ther Methods*. 2014;25(6):317–327.
17. Miccio A, et al. In vivo selection of genetically modified erythroblastic progenitors leads to long-term correction of β-thalassemia. *Proc Natl Acad Sci U S A*. 2008;105(30):10547–10552.
18. Zhao H, Pestina TI, Nasimuzzaman M, Mehta P, Hargrove PW, Persons DA. Amelioration of murine β-thalassemia through drug selection of hematopoietic stem cells transduced with a lentiviral vector encoding both γ-globin and the MGMT drug-resistance gene. *Blood*. 2009;113(23):5747–5756.
19. Cavazzana-Calvo M, et al. Gene therapy of human severe combined immunodeficiency (SCID)-X1 disease. *Science*. 2000;288(5466):669–672.
20. Gaspar HB, et al. Hematopoietic stem cell gene therapy for adenosine deaminase-deficient severe combined immunodeficiency leads to long-term immunological recovery and metabolic correction. *Sci Transl Med*.

2011;3(97):97ra80.
21. Aiuti A, et al. Lentiviral hematopoietic stem cell gene therapy in patients with Wiskott-Aldrich syndrome. *Science*. 2013;341(6148):1233151.
22. Persons DA, Allay ER, Sabatino DE, Kelly P, Bodine DM, Nienhuis AW. Functional requirements for phenotypic correction of murine β-thalassemia: implications for human gene therapy. *Blood*. 2001;97(10):3275–3282.
23. Andreani M, et al. Persistence of mixed chimerism in patients transplanted for the treatment of thalassemia. *Blood*. 1996;87(8):3494–3499.
24. Negre O, et al. Correction of murine β-thalassemia after minimal lentiviral gene transfer and homeostatic in vivo erythroid expansion. *Blood*. 2011;117(20):5321–5331.
25. McColl B, Vadolas J. Animal models of β-hemoglobinopathies: utility and limitations. *J Blood Med*. 2016;7:263–274.
26. Pestina TI, Hargrove PW, Jay D, Gray JT, Boyd KM, Persons DA. Correction of murine sickle cell disease using γ-globin lentiviral vectors to mediate high-level expression of fetal hemoglobin. *Mol Ther*. 2009;17(2):245–252.
27. Zielske SP, Lingas KT, Li Y, Gerson SL. Limited lentiviral transgene expression with increasing copy number in an MGMT selection model: lack of copy number selection by drug treatment. *Mol Ther*. 2004;9(6):923–931.
28. Abkowitz JL, Catlin SN, McCallie MT, Guttorp P. Evidence that the number of hematopoietic stem cells per animal is conserved in mammals. *Blood*. 2002;100(7):2665–2667.
29. Chen J, Larochelle A, Fricker S, Bridger G, Dunbar CE, Abkowitz JL. Mobilization as a preparative regimen for hematopoietic stem cell transplantation. *Blood*. 2006;107(9):3764–3771.
30. Brousse V, Buffet P, Rees D. The spleen and sickle cell disease: the sick(led) spleen. *Br J Haematol*. 2014;166(2):165–176.
31. Zhang W, et al. Integration profile and safety of an adenovirus hybrid-vector utilizing hyperactive sleeping beauty transposase for somatic integration. *PLoS One*. 2013;8(10):e75344.
32. Wang H, et al. A capsid-modified helper-dependent adenovirus vector containing the β-globin locus control region displays a non-random integration pattern and allows stable, erythroid-specific gene expression. *J Virol*. 2005;79(17):10999–11013.
33. Li C, et al. Reactivation of γ-globin in adult β-YAC mice after ex vivo and in vivo hematopoietic stem cell genome editing. *Blood*. 2018;131(26):2915–2928.
34. Arcasoy MO, Romana M, Fabry ME, Skarpidi E, Nagel RL, Forget BG. High levels of human γ-globin gene expression in adult mice carrying a transgene of deletion-type hereditary persistence of fetal hemoglobin. *Mol Cell Biol*. 1997;17(4):2076–2089.
35. Nishino T, Cao H, Stamatoyannopoulos G, Emery DW. Effects of human γ-globin in murine β-thalassaemia. *Br J Haematol*. 2006;134(1):100–108.
36. Weatherall DJ. Thalassemia. In: Stamatoyannopolous G, et al., eds. *The Molecular Basis of Blood Disorders*. 3rd ed. Philadelphia, Pennsylvania, USA: WB Saunders; 2001:183–226.
37. Karponi G, et al. Plerixafor+G-CSF-mobilized CD34$^+$ cells represent an optimal graft source for thalassemia gene therapy. *Blood*. 2015;126(5):616–619.
38. Karpova D, et al. Continuous blockade of CXCR4 results in dramatic mobilization and expansion of hematopoietic stem and progenitor cells. *Blood*. 2017;129(21):2939–2949.
39. Ni S, Bernt K, Gaggar A, Li ZY, Kiem HP, Lieber A. Evaluation of biodistribution and safety of adenovirus vectors containing group B fibers after intravenous injection into baboons. *Hum Gene Ther*. 2005;16(6):664–677.
40. Ong HT, et al. Oncolytic measles virus targets high CD46 expression on multiple myeloma cells. *Exp Hematol*. 2006;34(6):713–720.
41. Atasheva S, Shayakhmetov DM. Adenovirus sensing by the immune system. *Curr Opin Virol*. 2016;21:109–113.
42. Greig JA, et al. Impact of intravenous infusion time on AAV8 vector pharmacokinetics, safety, and liver transduction in cynomolgus macaques. *Mol Ther Methods Clin Dev*. 2016;3:16079.
43. Seregin SS, et al. Transient pretreatment with glucocorticoid ablates innate toxicity of systemically delivered adenoviral vectors without reducing efficacy. *Mol Ther*. 2009;17(4):685–696.
44. Illingworth S, et al. Preclinical safety studies of enadenotucirev, a chimeric group b human-specific oncolytic adenovirus. *Mol Ther Oncolytics*. 2017;5:62–74.
45. Garcia-Carbonero R, et al. Phase 1 study of intravenous administration of the chimeric adenovirus enadenotucirev in patients undergoing primary tumor resection. *J Immunother Cancer*. 2017;5(1):71.
46. Neff T, et al. Methylguanine methyltransferase-mediated in vivo selection and chemoprotection of allogeneic stem cells in a large-animal model. *J Clin Invest*. 2003;112(10):1581–1588.
47. Li C, et al. Reactivation of γ-globin in adult β-YAC mice after ex vivo and in vivo hematopoietic stem cell genome editing. *Blood*. 2018;131(26):2915–2928.
48. Radtke S, et al. A distinct hematopoietic stem cell population for rapid multilineage engraftment in nonhuman primates. *Sci Transl Med*. 2017;9(414):eaan1145.
49. Beard BC, et al. Long-term polyclonal and multilineage engraftment of methylguanine methyltransferase P140K gene-modified dog hematopoietic cells in primary and secondary recipients. *Blood*. 2009;113(21):5094–5103.
50. Lek M, et al. Analysis of protein-coding genetic variation in 60,706 humans. *Nature*. 2016;536(7616):285–291.
51. Li C, et al. Integrating HDAd5/35++ vectors as a new platform for HSC gene therapy of hemoglobinopathies. *Mol Ther Methods Clin Dev*. 2018;9:142–152.
52. Deyle DR, Russell DW. Adeno-associated virus vector integration. *Curr Opin Mol Ther*. 2009;11(4):442–447.
53. Bartholomae CC, et al. Lentiviral vector integration profiles differ in rodent postmitotic tissues. *Mol Ther*. 2011;19(4):703–710.
54. Schröder AR, Shinn P, Chen H, Berry C, Ecker JR, Bushman F. HIV-1 integration in the human genome favors active genes and local hotspots. *Cell*. 2002;110(4):521–529.
55. Li C, Gil S, Sova P, Valensisi C, Lieber A. HDAd5/35++-mediated targeted integration in HSCs of AAVS1 transgenic mice results in efficient transgene marking in peripheral blood mononuclear cells. 21st Annual American Society of Gene and Cell Therapy Meeting. Abstract 972. https://www.cell.com/molecular-therapy-family/molecular-therapy/pdf/S1525-0016(18)30204-1.pdf?_returnURL=https%3A%2F%2Flinkinghub.elsevier.com%2Fretrieve%2Fpii%2FS1525001618302041%3Fshowall%3Dtrue. Accessed December 3, 2018.
56. Tuve S, et al. A new group B adenovirus receptor is expressed at high levels on human stem and tumor cells. *J Virol*. 2006;80(24):12109–12120.
57. Harworth KG, Atkins MA, Richter M, Peterson CW, Lieber A, HP K. Direct in vivo transduction of mobilized CD34 HSPCs with adenoviral vectors in non-human primates. 21st Annual American Society of Gene and Cell Therapy Meeting. Abstract 995. https://www.cell.com/molecular-therapy-family/molecular-therapy/pdf/S1525-0016(18)30204-1.pdf?_returnURL=https%3A%2F%2Flinkinghub.elsevier.com%2Fretrieve%2Fpii%2FS1525001618302041%3Fshowall%3Dtrue. Accessed December 3, 2018.
58. Vogels R, et al. Replication-deficient human adenovirus type 35 vectors for gene transfer and vaccination: efficient human cell infection and bypass of preexisting adenovirus immunity. *J Virol*. 2003;77(15):8263–8271.
59. Abbink P, et al. Comparative seroprevalence and immunogenicity of six rare serotype recombinant adenovirus vaccine vectors from subgroups B and D. *J Virol*. 2007;81(9):4654–4663.
60. Kostense S, et al. Adenovirus types 5 and 35 seroprevalence in AIDS risk groups supports type 35 as a vaccine vector. *AIDS*. 2004;18(8):1213–1216.
61. Flomenberg PR, Chen M, Munk G, Horwitz MS. Molecular epidemiology of adenovirus type 35 infections in immunocompromised hosts. *J Infect Dis*. 1987;155(6):1127–1134.
62. Barouch DH, et al. International seroepidemiology of adenovirus serotypes 5, 26, 35, and 48 in pediatric and adult populations. *Vaccine*. 2011;29(32):5203–5209.
63. Johnson MJ, et al. Type I IFN induced by adenovirus serotypes 28 and 35 has multiple effects on T cell immunogenicity. *J Immunol*. 2012;188(12):6109–6118.
64. Adams WC, Berenson RJ, Karlsson Hedestam GB, Lieber A, Koup RA, Loré K. Attenuation of CD4$^+$ T-cell function by human adenovirus type 35 is mediated by the knob protein. *J Gen Virol*. 2012;93(pt 6):1339–1344.
65. Adams WC, et al. Adenovirus type-35 vectors block human CD4$^+$ T-cell activation via CD46 ligation. *Proc Natl Acad Sci U S A*. 2011;108(18):7499–7504.
66. Shoji M, Yoshizaki S, Mizuguchi H, Okuda K, Shimada M. Immunogenic comparison of chimeric adenovirus 5/35 vector carrying optimized human immunodeficiency virus clade C genes and various promoters. *PLoS One*. 2012;7(1):e30302.
67. Sakurai F, et al. Adenovirus serotype

35 vector-mediated transduction into human CD46-transgenic mice. *Gene Ther*. 2006;13(14):1118–1126.
68. Sakurai F, et al. Transduction properties of adenovirus serotype 35 vectors after intravenous administration into nonhuman primates. *Mol Ther*. 2008;16(4):726–733.
69. Baden LR, et al. Assessment of the safety and immunogenicity of 2 novel vaccine platforms for HIV-1 prevention: a randomized trial. *Ann Intern Med*. 2016;164(5):313–322.
70. Kazmin D, et al. Systems analysis of protective immune responses to RTS,S malaria vaccination in humans. *Proc Natl Acad Sci U S A*. 2017;114(9):2425–2430.
71. Palmer D, Ng P. Methods for production of helper-dependent adenoviral vectors. In: Le Doux JM, ed. *Gene Therapy Protocols. Volume 1: Production and In Vivo Applications of Gene Transfer Vectors (Methods in Molecular Biology)*. 3rd ed. Totowa, New Jersey, USA: Humana Press; 2009:33–53.
72. Wang H, et al. In vitro and in vivo properties of adenovirus vectors with increased affinity to CD46. *J Virol*. 2008;82(21):10567–10579.
73. Haeussler DJ, Evangelista AM, Burgoyne JR, Cohen RA, Bachschmid MM, Pimental DR. Checkpoints in adenoviral production: cross-contamination and E1A. *PLoS One*. 2011;6(8):e23160.